UNIVERSIDADE FEDERAL DE SÃO CARLOS
CENTRO DE CIÊNCIAS BIOLÓGICAS E DA SAÚDE
PROGRAMA DE PÓS-GRADUAÇÃO EM ECOLOGIA E RECURSOS NATURAIS

NATÁLIA CANTUÁRIA DA SILVA

PURPOSES AND CHOISES ON THE CHARACTERIZATION OF FOSSIL SAMPLES: PARAMETER TEST AND ANALYTICAL TECHNIQUES APPLIED TO THE COMPARISON OF DIFFERENT SUBSTRATES

SÃO CARLOS - SP
2022

NATÁLIA CANTUÁRIA DA SILVA

PURPOSES AND CHOISES ON THE CHARACTERIZATION OF FOSSIL SAMPLES: PARAMETER TEST AND ANALYTICAL TECHNIQUES APPLIED TO THE COMPARISON OF DIFFERENT SUBSTRATES

Dissertação apresentada ao Programa de Pós-Graduação em Ecologia e Recursos Naturais da Universidade Federal de São Carlos, para obtenção do título de mestre em Ecologia e Recursos Naturais

Área de concentração: Ecologia e Recursos Naturais

Orientadora: Profª. Dra. Mírian Liza Alves Forancelli Pacheco

SÃO CARLOS - SP
2022

UNIVERSIDADE FEDERAL DE SÃO CARLOS

Centro de Ciências Biológicas e da Saúde
Programa de Pós-Graduação em Ecologia e Recursos Naturais

Folha de Aprovação

Defesa de Dissertação de Mestrado da candidata Natália Cantuária da Silva, realizada em 15/03/2022.

Comissão Julgadora:

Profa. Dra. Mírian Liza Alves Forancelli Pacheco (UFSCar)

Prof. Dr. Marcelo Adorna Fernandes (UFSCar)

Prof. Dr. Rafael Delcourt de Seixas Ferreira (USP)

O Relatório de Defesa assinado pelos membros da Comissão Julgadora encontra-se arquivado junto ao Programa de Pós-Graduação em Ecologia e Recursos Naturais.

AGRADECIMENTOS

Agradeço à minha orientadora, Profa. Mírian Pacheco por seu apoio e orientação durante esse período.

Ao Programa de Pós-Graduação em Ecologia e Recursos Naturais (PPGERN) por todo o apoio durante o mestrado.

À CAPES pelo auxílio financeiro.

Ao Laboratório de Catodoluminescência, Universidade Federal do Pará (UFPA); Laboratório da Quimiosfera, Universidade de São Paulo (USP); Laboratório de Plasmas Tecnológicos, Universidade Estadual Paulista (UNESP, Sorocaba); Centro de Estudos em Petrologia e Geoquímica, Universidade Federal do Rio Grande do Sul (UFRGS); Instituto de Geociências, Universidade de São Paulo (USP) e o Laboratório Nacional de Luz Síncrotron, Centro Nacional de Pesquisa em Energia e Materiais (CNPEM).

RESUMO

Historicamente, a Paleontologia tem se preocupado com questões observacionais e explicativas sobre os fósseis. No entanto, com o avanço da ciência e da tecnologia, um novo campo se estruturou dentro dessa área: a Paleometria. Este esforço interdisciplinar busca entender como podemos usar um conjunto de técnicas para acessar informações e interpretar dados em registros fósseis. A compreensão das limitações e complementaridades entre as técnicas pode esclarecer propósitos e escolhas na pesquisa paleontológica. Apesar de sua contribuição, a Paleometria como ciência ainda precisa ser mais desenvolvida em termos técnicos. Aqui, analisamos sedimentos (areia e argila), rochas (siltito e arenito) e fósseis (plantas e insetos) para comparar e correlacionar padrões apresentados durante o uso das técnicas que podem facilitar o trabalho do pesquisador, como por exemplo, o uso de altas tensões relacionado ao uso de recobrimento, permite que possamos ver a amostra em maior profundidade durante o uso do Microscópio Eletrônico de Varredura (MEV), assim como também foi observado que o aumento gradativo das tensões está relacionado a uma maior detecção de elementos na Espectroscopia de Energia Dispersiva (EDS), bem como sua correlação com os elementos-traço encontrados na Fluorescência de Raios-X (XRF).

Palavras-chave: Paleometria; Metodologias em paleontologia; Dados paleontológicos

ABSTRACT

Historically, paleontology has been concerned with observational and explanatory issues regarding fossils. However, with the advancement of science and technology, a new field has been structured within this area: paleometry. This interdisciplinary effort seeks to understand how we can use a bulk of techniques in order to access information and interpret data on fossil record. The understanding of limitations and complementarities among techniques can clarify purposes and choices in paleontological research. Despite its contribution, paleometry as a science still needs to be further developed in technical terms. Here, we analyze sediments (sand and clay), rocks (siltstone and sandstone) and fossils (plants and insects) to compare and correlate patterns presented during the use of techniques that can facilitate the researcher's work, such as the use of high tensions related to the use of coating that allows us to see the sample in greater depth during the use of the Scanning Electron Microscope (SEM), as well as observations that the gradual increase in tensions is related to a greater detection of elements in the Spectroscopy of Dispersive Energy (EDS) and its correlation with trace elements found in X-Ray Fluorescence (XRF).

Keywords: Paleometry; Methodologies in paleontology; Paleontological data

SUMÁRIO

INTRODUÇÃO

1.1. Algumas considerações sobre o Permiano no mundo e no Brasil

Durante o Paleozoico, glaciações e deglaciações modificaram sistemas físicos, químicos e biológicos na Terra, causando mudanças climáticas extremas (Isbell et al., 2012; Isbell et al., 2018). O período compreendido entre o Carbonífero e o Permiano encerra esse ciclo com uma deglaciação que resultou em um paleoambiente desértico (Poulsen et al., 2007). Para além desses fatos, episódios de transgressão e regressão marinha estão aliados a esses eventos e deixaram suas marcas no Brasil (Ng et al., 2019).

Por mais que esses eventos possuam sua devida importância é imprescindível não deixar de falar de extinção quando se trata do Permiano. A Grande Extinção em Massa do Permiano foi devastadora, extinguindo cerca de, aproximadamente, 95% das espécies aquáticas (Benton e Twitchett, 2003) bem como, aproximadamente, 89% das espécies terrestres (Benton e Newell, 2014).

Nesse contexto, o Brasil possui diversas evidências desse período tão enigmático na história da Terra. Especificamente, em Angatuba, no estado de São Paulo, afloram rochas da Formação Corumbataí, intervalo próximo do limite Permo-Triássico (Rocha-Campos et al., 2019). Essa formação apresenta icnofósseis (e.g. *Planolites, Skolithos* e *Palaeophycus*), e é rica em conchas de bivalves (coquinas) e caules de licófitas (*Lycopodiopsis derbyi*) preservados principalmente em arenitos e siltitos e já foram objetos de estudos para algumas interpretações paleoambientais que resultaram na descrição de um ambiente energético (Sallun Filho et al., 2012; Spiekermann et al., 2020).

1.2. Paleometria: introdução do manuscrito

Originalmente, a paleontologia é uma ciência histórica, observacional e explicativa, que passou por algumas revoluções teóricas, principalmente em sua esfera biológica (Sepkoski, 2008). No entanto, só recentemente os paleontólogos repensaram as abordagens metodológicas usadas para acessar informações e interpretação dos dados do registro fóssil na Terra (Orr et al., 2009; Bertrand et al., 2015; Gueriau et al., 2015; 2018; 2020 ; Marshall e Marshall, 2015; Foucher, 2019),

e como resultado, em outros mundos do Sistema Solar (Brasier e Wacey, 2012; Schopf et al., 2012). Essa revolução metodológica é conhecida como paleometria (Riquelme et al., 2009). Embora alguns artigos já tenham utilizado este termo (Delgado et al., 2014; Gomes et al., 2019), devido aos seus objetivos principais, definimos a paleometria como um esforço interdisciplinar que visa propor, desenvolver ou aprimorar formas cada vez mais eficazes e eficientes de acesso à informação, bem como compilação e interpretação dos dados do registro fóssil.

A paleometria tem promovido avanços consideráveis nos seguintes problemas: (1) revisão e estabelecimento de novos critérios de biogenicidade; (2) reconhecimento de contextos viáveis para a vida; e (3) desenvolvimento de novas técnicas que permitem o acesso e interpretação dos dados (Brasier e Wacey, 2012).

Assim, o desenvolvimento e o aprimoramento de técnicas de acesso às informações paleobiológicas e astrobiológicas caminham lado a lado com os avanços da física aplicada. Descobertas recentes integradas com formas cada vez mais sofisticadas de investigar e testar hipóteses no registro fóssil (por exemplo, Schopf et al., 2012) permitiram a revisão de conceitos e entendimentos de questões importantes, como os limites da biosfera da Terra e habitabilidade em outros mundos (Hutchinson et al., 2014; Grotzinger, 2014; Dodd et al., 2017; Orosei et al., 2018).

Neste contexto, áreas específicas da paleontologia, como fossildiagênese (Osés et al., 2016; 2017, Becker-Kerber et al., 2017; Barros et al., 2019; Dias e Carvalho, 2020), e tafonomia experimental (Iniesto et al., 2017, 2018, 2021; Gomes et al., 2019), acabam se beneficiando e também contribuindo com testes de parâmetros analíticos importantes para estudos mais detalhados sobre o registro fóssil.

Em escalas micro e ultraestruturais, o uso combinado de técnicas espectroscópicas e espectrométricas, tem permitido a caracterização e a investigação de diferentes processos e padrões de preservação de organismos (Wiemann e Briggs, 2021; Jiménez et al., 2021) em diferentes estágios da diagênese (por exemplo, Trueman, 2013).

O registro fóssil brasileiro também se beneficiou do desenvolvimento combinado e aplicações de técnicas paleométricas (Osés et al., 2016, 2017; Gomes

et al., 2019; Becker-Kerber et al., 2020, 2021). No entanto, muitas questões relacionadas à fossildiagênese e geobiologia permanecem abertas para uma série de fósseis, nos mais diversos contextos de preservação, e podem ser respondidas com base em refinamentos metodológicos paleométricos.

A investigação sobre os limites das técnicas analíticas aplicadas ao estudo de materiais geológicos pode ser realizada testando combinações de parâmetros específicos em diferentes tipos de preparações de amostras. A clareza dos propósitos investigativos e o conhecimento dos limites e restrições sobre uma técnica permitem um bom desenho experimental/analítico e escolha adequada de técnicas complementares (também com limites bem conhecidos). Isso resulta na recuperação de dados mais robustos no registro geológico.

Diante do exposto, o manuscrito apresentado nessa dissertação tem como objetivo apresentar alguns resultados de testes de diferentes técnicas analíticas, sob diversos parâmetros, na análise de sedimentos, rochas e fósseis

ARTIGO SUBMETIDO: Purposes and choices on the characterization of fossil samples: parameter tests and analytical techniques applied to the comparison of different substrates

(Artigo submetido para a *Journal of South American Earth Sciences)*

Natália Cantuária [1,2], Lucas D. Mouro [3,4], Mírian L. A. F. Pacheco [2,5]

[1] Programa de Pós-Graduação em Ecologia e Recursos Naturais (PPGERN), Universidade Federal de São Carlos (UFSCar - campus São Carlos), São Carlos - SP, Brazil.

[2] Laboratório de Estudos Paleobiológicos (LEPBio), Departamento de Biologia, Universidade Federal de São Carlos (UFSCar - campus Sorocaba), CCHB-1112, Sorocaba - SP, Brazil.

[3] Pós-Graduação em Geologia, Departamento de Geologia, Universidade Federal de Santa Catarina (UFSC), PFRH-PB 240, Florianópolis - SC, 88040-900, Brazil.

[4] Departamento de Geologia e Paleontologia, Museu Nacional/Universidade Federal Rio de Janeiro (UFRJ), Rio de Janeiro - RJ, 20940-040, Brazil.

[5] Instituto de Física (IF), Universidade de São Paulo (USP), Cidade Universitária, São Paulo – SP, Brazil.

Abstract. Historically, paleontology has been concerned with observational and explanatory issues regarding fossils. However, with the advancement of science and technology, a new field has been structured within this area: paleometry. This interdisciplinary effort seeks to understand how we can use a bulk of techniques in order to access information and interpret data on fossil record. The understanding of limitations and complementarities among techniques can clarify purposes and choices in paleontological research. Despite its contribution, paleometry as a science still needs to be further developed in technical terms. This article aims to present some results of tests of different analytical techniques, under different parameters, in the analysis of sediments, rocks, and fossils.

Keywords: Paleometry; Methodologies in paleontology; Paleontological data

Highlights:

- Purposes and choices are crucial issues in order to choose adequate techniques applied to the characterization of geological samples.
- Understanding the limitations and complementarities of different techniques can help to obtain more objective and robust data on paleontology.
- Paleometry can be an important tool for basic science research in geosciences.

1. Introduction

Originally, paleontology is a historical observational, and explanatory science, which has undergone some theoretical revolutions, mainly in its biological sphere (Sepkoski, 2008). However, it is only recently that paleontologists have rethought the methodological approaches used to access information and interpretation of data from Earth fossil record (Orr et al., 2009; Bertrand et al., 2015; Gueriau et al., 2015; 2018; 2020; Marshall and Marshall, 2015; Foucher, 2019), and as a result, from other rocky worlds in the Solar System (Brasier and Wacey, 2012; Schopf et al., 2012).

This methodological revolution is known as paleometry (Riquelme et al., 2009). Although some articles have already used this term (Delgado et al., 2014; Gomes et al., 2019), due to its main objectives, we define paleometry as an interdisciplinary effort that aims to propose, develop or improve increasingly effective and efficient forms of access of information, as well as compilation and interpretation of data in the fossil record.

Paleometry has promoted considerable advances in the following issues: (1) revision and establishment of new biogenicity criteria; (2) recognition of viable contexts for life; and (3) development of new techniques that allow access and interpretation of data (Brasier and Wacey, 2012).

Thus, the development and improvement of techniques for accessing paleobiological and astrobiological information go hand in hand with advances in applied physics. Discoveries integrated with increasingly sophisticated ways of investigating and testing hypotheses in the fossil record (e.g., Schopf et al., 2012) have allowed the revision of concepts and understandings of major issues such as

the limits of the Earth's biosphere and habitability in other worlds (Hutchinson et al., 2014; Grotzinger, 2014; Dodd et al., 2017; Orosei et al., 2018).

In this context, specific areas of paleontology, such as diagenesis of fossils (Osés et al., 2016; 2017, Becker-Kerber et al., 2017; Barros et al., 2019; Dias and Carvalho, 2020), and experimental taphonomy (Iniesto et al., 2017, 2018, 2021; Gomes et al., 2019), end up both benefiting and also contributing to tests of important analytical parameters for more detailed studies on the fossil record.

At micro and ultrastructural scales, the combined use of techniques such as spectroscopic and spectrometric, has allowed the characterization and investigations into different processes and patterns of preservation of organisms (Wiemann and Briggs, 2021; Jiménez et al., 2021) at different stages of diagenesis (e.g., Trueman, 2013).

The Brazilian fossil record has also benefited from the combined development and applications of paleometric techniques (Osés et al., 2016, 2017; Gomes et al., 2019; Becker-Kerber et al., 2020, 2021). However, many questions related to diagenesis and geobiology remain open for a series of fossils, in the most diverse preservation contexts, and can be answered based on paleometric methodological refinements.

The investigation of the limits of analytical techniques, applied to the study of geological materials can be carried out by testing combinations of specific parameters under different sample preparations. The clarity of investigative purposes and knowledge about the limits and restrictions of a technique allows a good experimental/analytical design and the adequate choice of complementary techniques (with also well-known limits). This results in the retrieval of more robust data on the geological record.

Given the above, this article aims to present some results provided by tests of different analytical techniques, under different parameters, in the analysis of sediments, rocks, and fossils.

2. Samples

We chose to analyze two different types of pure sediments and two types of related lithologies containing fossils. The chosen sediments were: pure washed fine

to medium sand fraction (quartz) and pure clay illite. The analyzed fossils were: fragments of plant stems preserved in fine sandstone/siltite and insects preserved in bituminous shales.

Sands are a pre-washed natural quartz substrate obtained from a store specialized in aquarium products. Clays were donated by “Minérios Ouro Branco Ltda”.

The silicified stem fragments were collected on outcrops from the Corumbataí Formation (Permian, Passa Dois Group) at Angatuba, São Paulo State, Brazil (Figure 1). This geological unity is mainly composed of intercalated sand-, silt- and mudstones (Fúlfaro, 1970), where is common to find, among other fossils, plant stems (de Faria et al., 2009; Spiekermann et al., 2020).

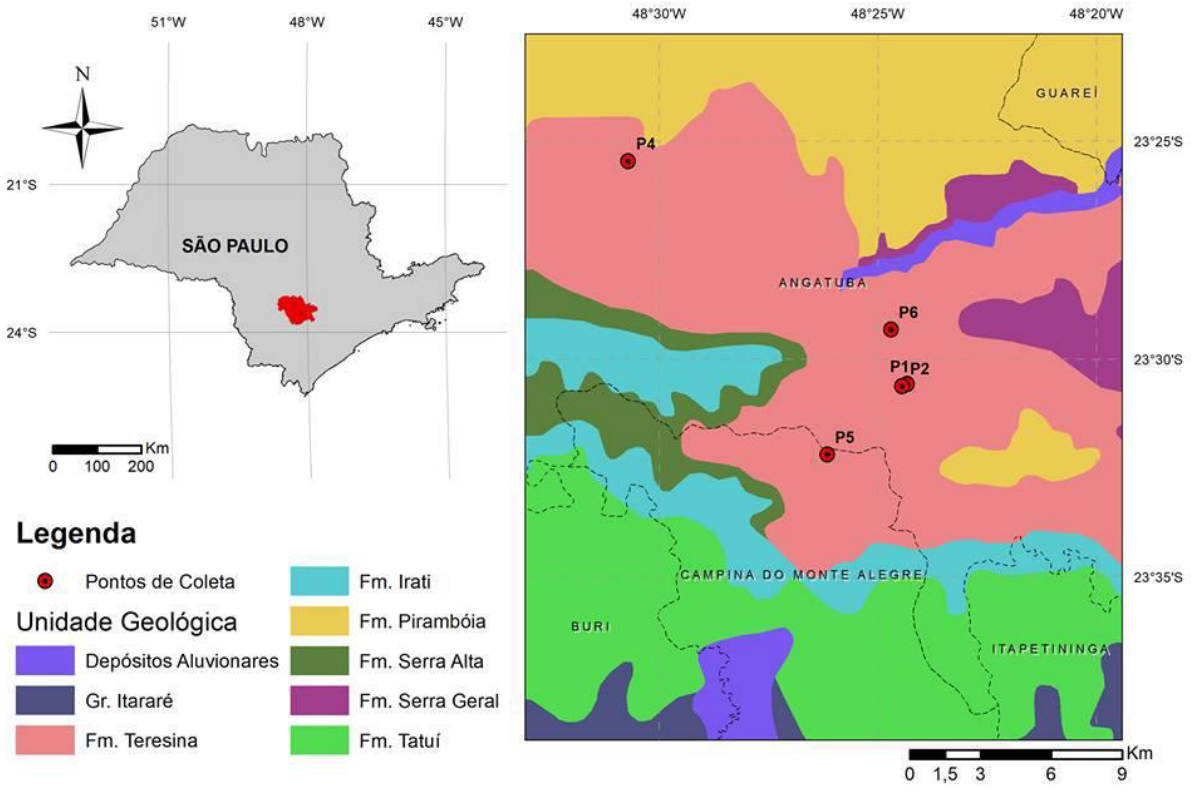

Figure 1. Map from the city of Angatuba inside São Paulo State. Created by Gabriel Barros.

The fossil insects are preserved in the Lontras Shale (Upper Carboniferous, Itararé Group, Paraná Basin) from Mafra, Santa Catarina State, Brazil (Figure 2),

which is composed of siltstones, mudstone packages and varved shales (Mouro et al., 2020).

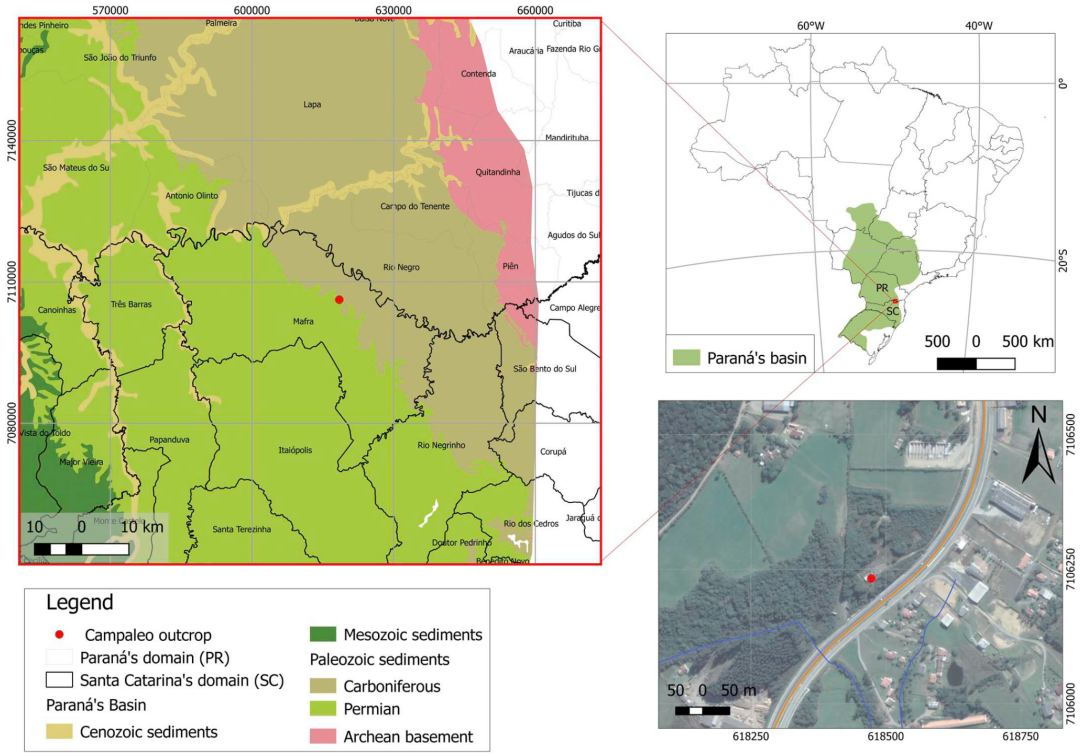

Figure 2. Map of Lontras Shale. Taken from Mouro et al. (2020).

Sand and clay served as a homogeneous substrate control for testing parameters and different techniques, free of impurities and minerals (other than pure quartz and illite) related to the fossilization process. Fossils from distinct lithologies were used in order to compare the effectiveness of different techniques and parameters on heterogeneous samples (other than sand and clay) with different preservation modes.

3. Used Techniques and data compilation

3.1. Scanning Electron Microscopy with Energy Dispersive Spectroscopy (SEM/EDS), Cathodoluminescence and Micro-X-ray fluorescence (μXRF)

Cathodoluminescence, SEM/EDS and XRF are very effective, with well-established applications in several scientific areas, and they are widely used in

geosciences. These techniques have advantageous features such as the ability to perform morphologic, topographic and petrographic analysis (microscopy), identifying elements at different spots over small areas. This allows comparisons between chemical composition from various locations in the same sample and/or among samples (Wagner, 1999; Brouwer, 2010; Figueiredo et al., 2011).

Fossils are almost always heterogeneous materials (a mixture of minerals and organic matter) preserved in heterogeneous substrates (sedimentary rocks). We should always keep this in mind hence, the lack of knowledge about the specificities of the samples under study can lead to the wrong choice or misuse of predefined standards. Even the issue under investigation can influence the choice of standards: surficial morphology, topography, amount of organic matter etc.

In the case of SEM/EDS, for example, the use of lower electric tensions (3 to 5keV) may be suitable for identifying thin organic films or clay minerals covering specimens. On the other hand, higher electric tensions (from 15keV on) may reveal heavier elements, which are important for diagenesis investigation, such as Sr and Rare Earths Elements (REE), but which may be in trace forms.

In this sense, the recognition of parameters suitable for very specific geochemical characterizations, or even the identification of unique structures and textures, must be done under rigorous parameter tests.

The SEM-EDS techniques allow a general investigation of the samples, covering both lighter elements (such as C) and heavier ones (such as Fe). However, even the heaviest elements, when in low quantities (trace elements) may not have their intensities detected. In XRF analysis, the sensitivity to these heavier elements can be much higher. Given well-known limitations, these techniques can be complementary in many sample characterizations.

We used the JEOL JSM-6010 LA Scanning Electron Microscope (SEM), coupled with an Energy Dispersive Spectrometer (EDS), and a JEOL JSM-6610LV SEM equipped with a BRUKER Nano X flash detector 5030 EDS. These equipment were used for morphological and textural characterization as well as elementary chemical investigation of the samples.

To compare optimized parameters, part of the samples was covered using a DESK-V HP cold coating system. Since we investigated organic compounds and

minerals, all samples subjected to coating were covered with gold/palladium, and not carbon.

For better visual representation and comparisons between elementary heterogeneities, we present electron secondary images (SEI) and EDS mapping data. We chose the following electric tensions for the analyses: 3, 5, 10, 15, and 20 keV, with combinations of spot size ranging from 10, 20, 30, 40, 60, to 70.

EDS graphical representations were produced in the R (4.1.0) language using the integrated development environment RStudio (1.4.1717) and the 'ggplot2' (Wickham, 2011) package. R Scripts and raw data can be found in the Supplementary Material.

In order to complement EDS characterizations, we used the Synchrotron Light X-ray Micro-Fluorescence (micro-XRF) line from the Brazilian Center for Research in Energy and Materials (CNPEM, proposal 20190140). We performed the measurements using a 2 mm collimator, step 0,03. The maps were later processed with PyMca software

We applied hot cathodoluminescence imaging to compare with SEM micrographs, in order to obtain a wider view of the sediments, as well as to raise information regarding grains morphology, texture, overgrowths, zonations, inclusions and defects. This technique consists of an electromagnetic phenomena where the impact of electrons in a particular material results in the transference of energy from one ion to an activator ion, with emission of a photon causing the luminescence. Conversely, if the energy is transferred from an activator ion to another ion, the luminescence effect is attenuated or does not occur (Budd et al., 2000). The analyses were performed on an Mk5-2 CITL. The system was operated with an acceleration voltage between 15.6 and 16.2 kV, a current of 344 to 508 μA, and a vacuum between 0.05 and 0.003 Pa, with an exposure time of 10.2 to 17.2 s. Images were captured by a Leica DFC310 FX camera, coupled to a Leica DM4500P LED microscope, later processed in LAS V4.4 software. We used two thin polished sections mounted with balsam and minerals dispersed in fine to medium sand fraction (125–500μm). The sediments consisted of a mixture of rounded to angular grains, with a predominance of the latter.

3.2. X-ray diffraction and Micro-Raman Spectroscopy (μRaman)

Elementary techniques such as EDS and XRF reveal information about chemical elements from the innermost electronic layers of atoms. These techniques only allow the identification of elements. On the other hand, X-ray diffraction (XRD) and micro-Raman spectroscopy provide information about molecules. XRD reveals the crystal structure while Raman shows the differences between vibrational energy levels of compounds.

Almost all XRD equipment requires the processing of samples through maceration and pastille making. Therefore, a significant part of the samples is characterized in their mineralogical composition. However, the sample processing procedure makes specific point measurements unfeasible to perform, preventing the heterogeneity of the sample from being characterized. Almost no special preparation is required for the investigation of geological samples by Raman. This is made possible by the combined system of objectives, lasers and different powers of Raman spectroscopy. When used in combination, XRD and Raman can not only complement data obtained from elementary techniques such as EDS and XRF, but also serve as calibrators of each other's results.

We used a Renishaw InVia^{TM} micro-Raman spectroscope coupled with 532 and 785 nm lasers. Analyzes were performed in static mode, with a center raman shift at 750 cm^{-1}, contemplating a wider range of comparable characteristic peaks (both for minerals and for organic matter). Power settings varied between 25 and 50mW, under 50x objectives, with 30 accumulations of 2 seconds each. Lontras Shale analyses were performed in static mode with a 532 nm laser for organic and mineral phases and 633 and 785 nm to minerals and organic compounds as well. Intensities were 0.1 to 50% using 5 and 50x objectives and 30 accumulations of 1 second each.

We used the Windows®-based Raman Environment (WiRE) software for baseline subtraction and peak recognition. The database consulted to identify the characteristic peaks was the RRUFF database (Lafuente et al., 2015), in addition to spectra described by the specialized scientific literature.

The mineralogical composition was also determined by X-ray powder diffraction in a Bruker D8 diffractometer (Cu Kα, 40 kV, 40 mA, step 0.02 °, 153

s/step, scanning from 3 to 105 ° 2θ) at the *NAP Geoanalítica* Laboratory of the University of São Paulo. Qualitative analysis was performed with the Panalytical High Score 3.0 software and the Crystallographic Open Database (Grazulis et al., 2009).

4. Results

4.1. Scanning Electron Microscope (SEM)

4.1.1. Sediment

Between 3 and 10keV (Fig. 3A-C), the analysis of uncoated sand shows us definition of the grains, degrees of deformation and rounding, and surface details in topography (fractures, signs of abrasion etc) (specially until 5keV). While between 15 and 20keV (Fig. 3) there is loss of definition and surface characteristics of the grains by charging, but three-dimensionality is still highlighted. However, when the sands are coated, among all tensions it is possible to observe some surface details on the grains, but 10 and 15keV (Fig. 3) also show a certain depth through the different tones between the grains.

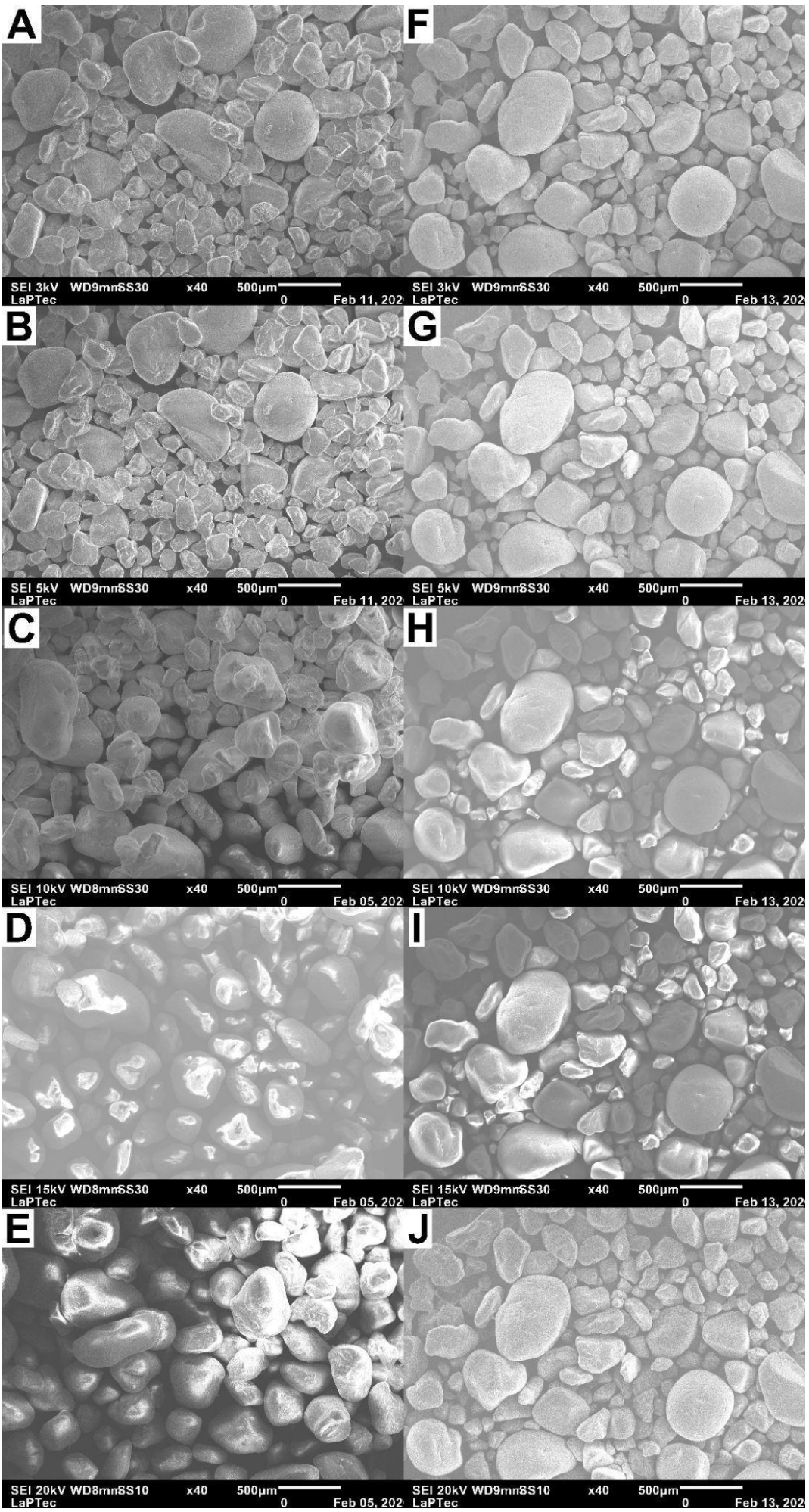
A
SEI 3kV WD9mm8S30 x40 500µm
LaPTec 0 Feb 11, 202
F
SEI 3kV WD9mm8S30 x40 500µm
LaPTec 0 Feb 13, 202
B
SEI 5kV WD9mm8S30 x40 500µm
LaPTec 0 Feb 11, 202
G
SEI 5kV WD9mm8S30 x40 500µm
LaPTec 0 Feb 13, 202
C
SEI 10kV WD8mm8S30 x40 500µm
LaPTec 0 Feb 05, 202
H
SEI 10kV WD9mm8S30 x40 500µm
LaPTec 0 Feb 13, 202
D
SEI 15kV WD8mm8S30 x40 500µm
LaPTec 0 Feb 05, 202
I
SEI 15kV WD9mm8S30 x40 500µm
LaPTec 0 Feb 13, 202
E
SEI 20kV WD8mm8S10 x40 500µm
LaPTec 0 Feb 05, 202
J
SEI 20kV WD9mm8S10 x40 500µm
LaPTec 0 Feb 13, 202

Figure 3. SEM micrographs of pure sand grains (quartz). In the first row we have uncoated sand from A to E at 3, 5, 10, 15 and 20keV, respectively. Note the surface of the uncoated grains missing surface details when the tensions are greater than 5keV. On the right side, from F to J, we show images of the coated sand at 3, 5, 10, 15 and 20keV, respectively. Here, in addition to visualizing the characteristics of the grains, we can also observe the topography of the grains that stand out in different shades, maintaining surface details. Scale bar = 500 μm. Magnification = x40. Spot size = 30 (A-D and F-I) and spot size = 10 (E and J).

The lowest tension, 3keV, in the uncoated clay sample, was not adequate for the analysis of this material as there is low visibility of the grains, however, the following tensions managed to pass, according to their increase, definition and individualization of grains, where we can observe the sharp grains of illite (Fig. 4B-E). The coated clay, as well as coated sand, made the grains not only visible and more defined, but it is also possible to observe differences among grain layers as the tension increases (Fig. 4G-J).

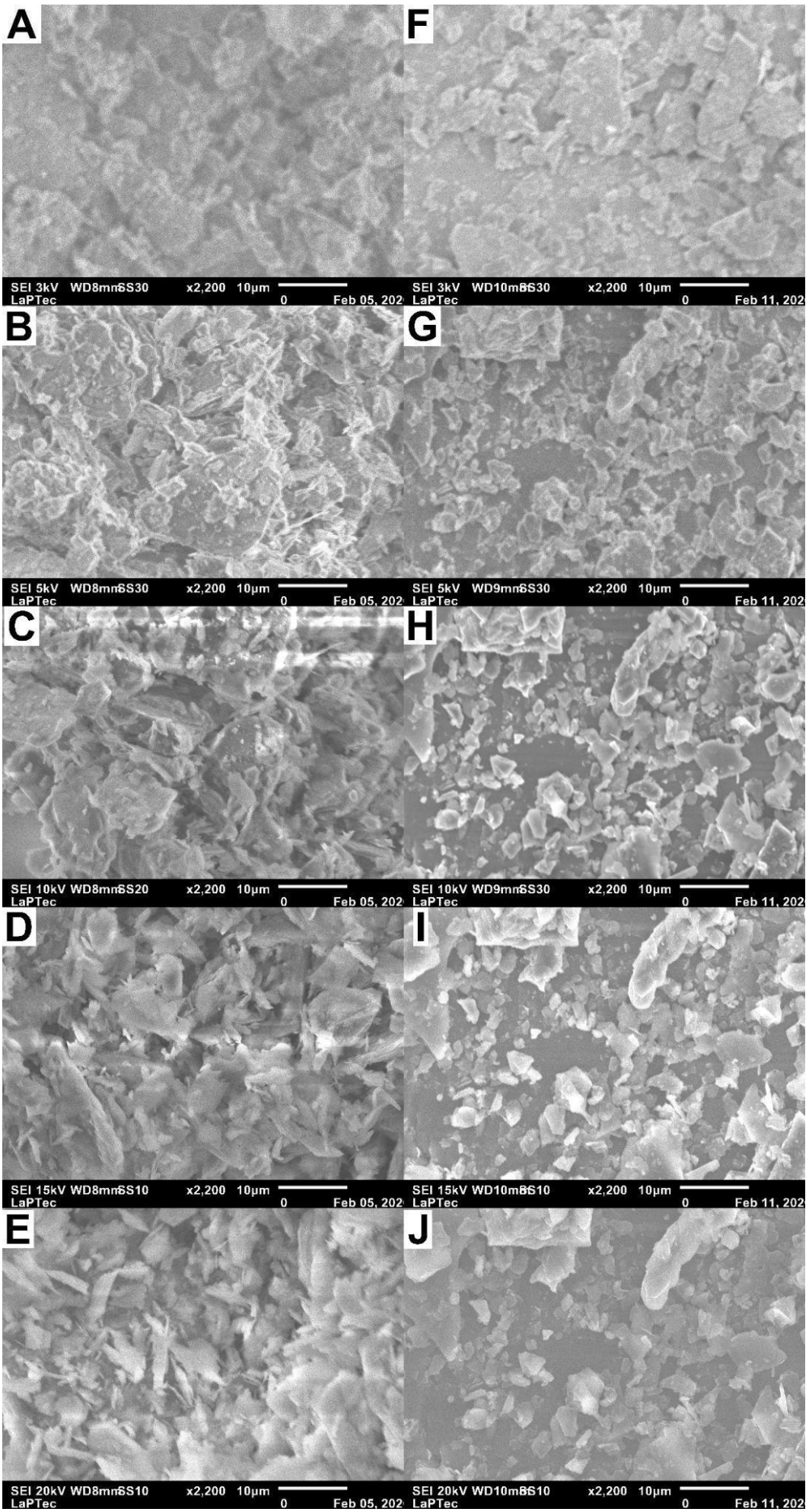
A
SEI 3kV WD8mm8S30 x2,200 10µm
LaPTec 0 Feb 05, 202
F
SEI 3kV WD10m8S30 x2,200 10µm
LaPTec 0 Feb 11, 202
B
SEI 5kV WD8mm8S30 x2,200 10µm
LaPTec 0 Feb 05, 202
G
SEI 5kV WD9mm8S30 x2,200 10µm
LaPTec 0 Feb 11, 202
C
SEI 10kV WD8mm8S20 x2,200 10µm
LaPTec 0 Feb 05, 202
H
SEI 10kV WD9mm8S30 x2,200 10µm
LaPTec 0 Feb 11, 202
D
SEI 15kV WD8mm8S10 x2,200 10µm
LaPTec 0 Feb 05, 202
I
SEI 15kV WD10m8S10 x2,200 10µm
LaPTec 0 Feb 11, 202
E
SEI 20kV WD8mm8S10 x2,200 10µm
LaPTec 0 Feb 05, 202
J
SEI 20kV WD10m8S10 x2,200 10µm
LaPTec 0 Feb 11, 202

Figure 4. SEM micrographs of pure clay (ilite) grains. In the first row we have uncoated clay (A to E) at tensions of 3, 5, 10, 15 and 20keV, respectively. Note the sharp morphology of the uncoated clay being clarified as tension increases. On the right side, from F to J, we have the coated clay at 3, 5, 10, 15 and 20keV, respectively. We can also observe here the different shades of gray highlighting grain layers regarding the depth of the analyzed coated grains. SEI = Secondary Electron Image. Scale bar = 10 μm. Spot size = 30 (A-B and F-H), 20 (C) and 10 (D-E and I-J). Magnification = x2,200.

When it comes to sediments, what we can observe is that the coated sample and high tensions can help to observe grain layers in depth and some superficial details. However, when we want to study surface grain details, it seems that the ideal is uncoated samples and lower tensions.

4.1.2. Fossil

As fossils are heterogeneous samples, we separated some regions of interest to analyze. Here, we show fragments of plant fossils from sand/silt levels of Corumbataí Formation, and insects preserved at Lontras Shale (Itararé Group).

The fragment of a silicified plant stalk was gold coated. We have observed a possible network of filaments of polymeric extracellular substances (EPS) linked to silicified minerals (Fig. 5A-B).

We have difficulties in observing mineral textures in tensions lower than 5 keV (Fig. 5A-B). In the case of possible EPS, indicated in green arrows (Fig. 5A-D, H), the web-like structure is more visible in higher tensions (especially at 15 keV), as the same time that thinner sheet-like structure (that is covering minerals), indicated in orange arrows (Fig. 5A-E, H), starts to disappear (Fig. 5D). Silicified minerals are more well defined in higher tensions (Fig. 5D-E).

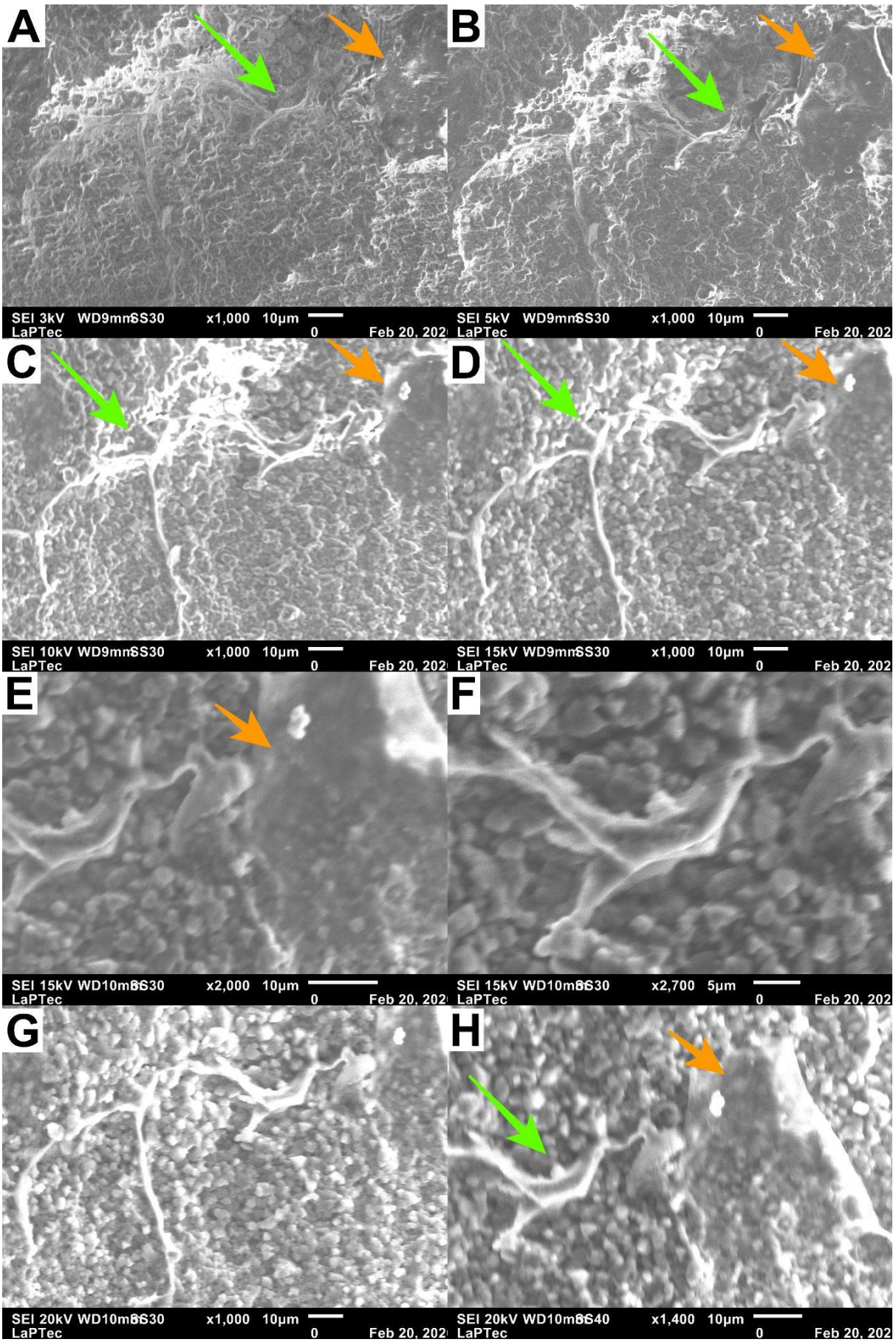
A
SEI 3kV WD9mm SS30 x1,000 10µm
LaPTec 0 Feb 20, 202
B
SEI 5kV WD9mm SS30 x1,000 10µm
LaPTec 0 Feb 20, 202
C
SEI 10kV WD9mm SS30 x1,000 10µm
LaPTec 0 Feb 20, 202
D
SEI 15kV WD9mm SS30 x1,000 10µm
LaPTec 0 Feb 20, 202
E
SEI 15kV WD10mm SS30 x2,000 10µm
LaPTec 0 Feb 20, 202
F
SEI 15kV WD10mm SS30 x2,700 5µm
LaPTec 0 Feb 20, 202
G
SEI 20kV WD10mm SS30 x1,000 10µm
LaPTec 0 Feb 20, 202
H
SEI 20kV WD10mm SS40 x1,400 10µm
LaPTec 0 Feb 20, 202

Figure 5. SEM micrographs of the lycopsid stem fragment from 3 to 20keV and spot size 30 and 40 (A-G, respectively). In the images it is possible to observe minerals and networks of a probable extracellular polymeric substance (EPS) in green arrows (A, B, C, D, H). It is also noted that, with the increase in tension, the closer and more visible the structures become which is indicated in orange arrows (A, B, C, D, E, H). SEI = Secondary Electron Image. Scale bar = 5 and 10 μm. Spot size = 30 and 40. Magnification = x1,000.

In general, fragments of lycopsids fossil tend to reveal more details about mineralogy in higher tensions (15 and 20 keV), as the same time as organic surface thin layers are not detected. However, at the same spot size, when we increase magnification (Fig. 6), we are able to observe more textural and morphological details even in tensions considered low for mineral detection (10 keV) when in lower magnifications. At the same time, thin surface organic matter is also detect at 10 keV (a tension considered too high for this structure at 10 keV). detailed in lower tensions, however, their composition of minerals and fossilized organic matter or morphological structures can bring different results not only taking into account tension but also other elements as spot size and magnification, as occurs in EPS (Figure 5B) and in the analysis of mineral morphology (Figure 6). In Figure 6, despite a 10keV tension, the grains show a great wealth of details about the mineral geometry.

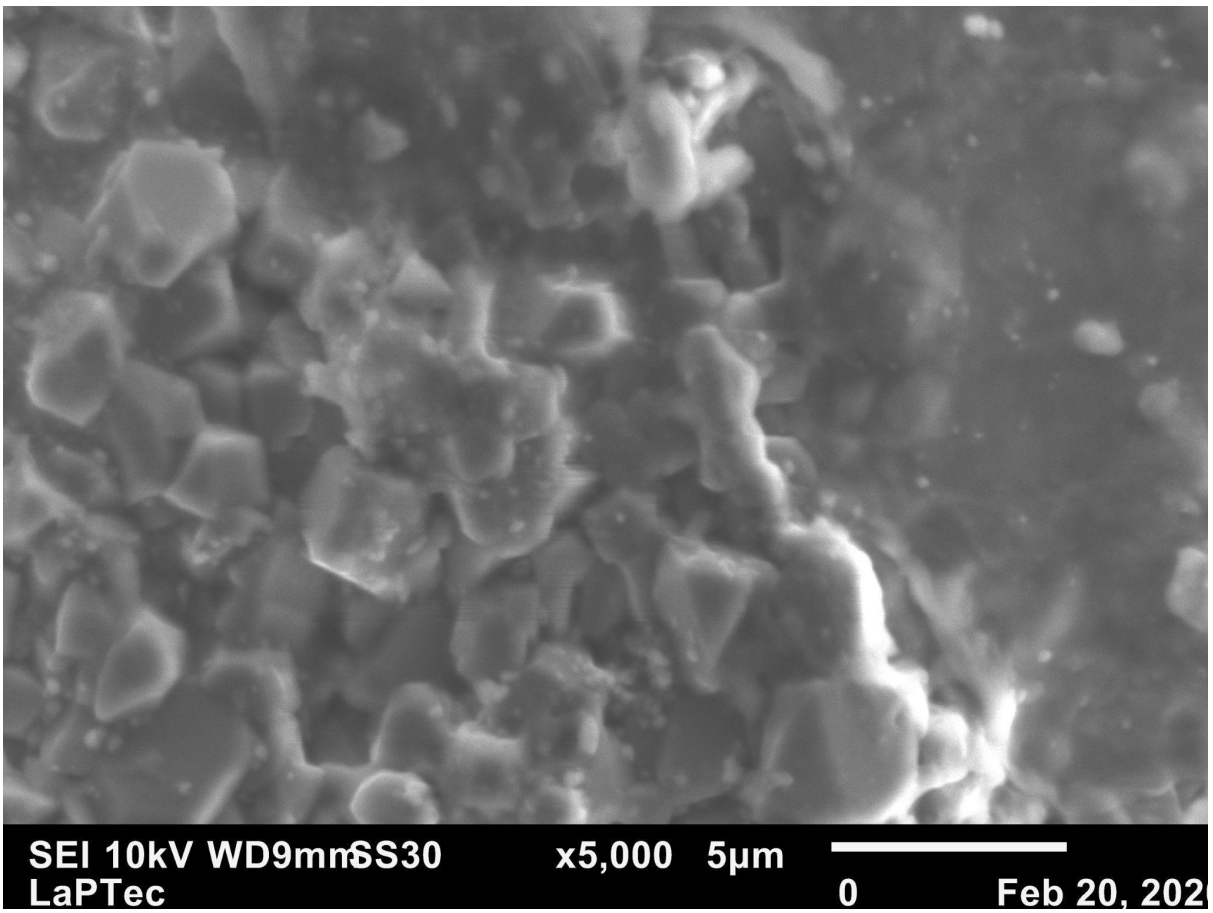

Figure 6. SEM micrograph of the lycopsid stem fragment at 10keV and spot size 30. During some tests with increasing magnification, we were able to observe more details in the minerals, including its euhedral geometry. SEI = Secondary Electron Image. Scale bar = 5 µm. Magnification = x5,000.

The same analyses were performed in some samples of fossil insects from Lontras Shale. Figure 5 shows a muscle fiber analyzed under tensions of 3 to 20keV without, also gold coated. Lower tensions are more favorable to show details in surface morphology and topography.

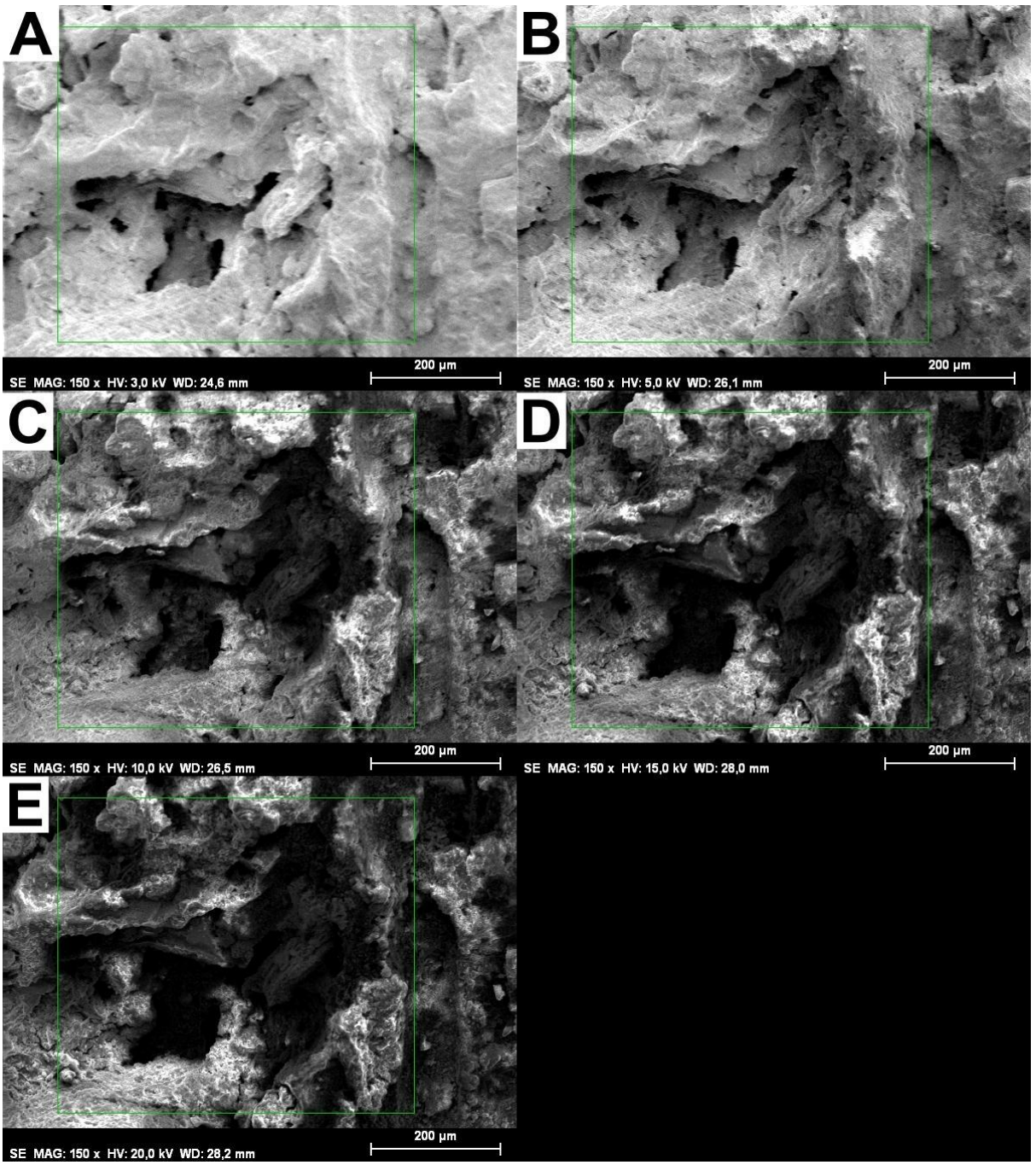

Figure 7. SEM micrographs of the muscle from Lontras Shale insect at 3 to 20keV (A-E, respectively). Note how the charging affects the lower (3keV) and higher tensions (15 and 20keV). Magnification = x150. Scale bar = 200 µm.

4.2. Energy Dispersive Spectroscopy (EDS) and Synchrotron Micro-X-Ray-Fluorescence (µXRF)

4.2.1. Sediment

The analysis of uncoated sand data shows, as expected, high intensities of O and Si, basic components of sand (Fig. 8A-C). Furthermore, it is observed that, as tensions are higher than 5 keV, , these elements become less detectable in some parts of the sample. At tensions higher than 15 keV, it is possible to detect C and Al (Figure 8D-E). In the case of coated sand, the elements became more intense as the beam penetrated the sample. We even detected lighter elements, as C, in lowest tensions (3keV), but we did not detected any elements other than O, Si and C in all tensions considered (Figure 9).

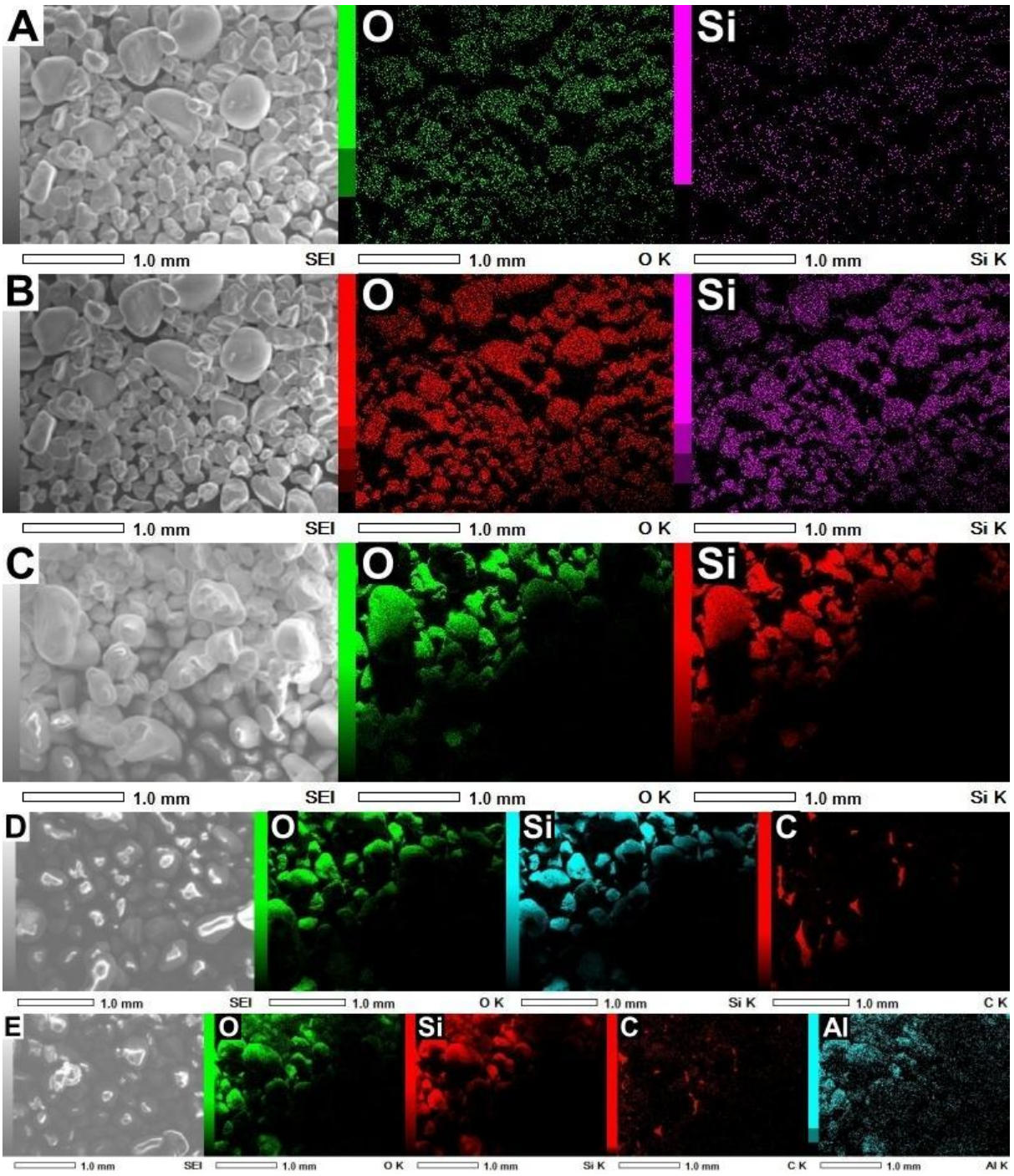

Figure 8. SEM/EDS of uncoated sand grains (A-E) from 3 to 20keV, respectively. Here, we can see how with increasing tension, there is greater detection of elements as the depth of the electron beam also increases. SEI = Secondary Electron Image. Scale bar = 1.0 mm. Spot size = 30 (A-D) and 10 (E). Magnification = x40.

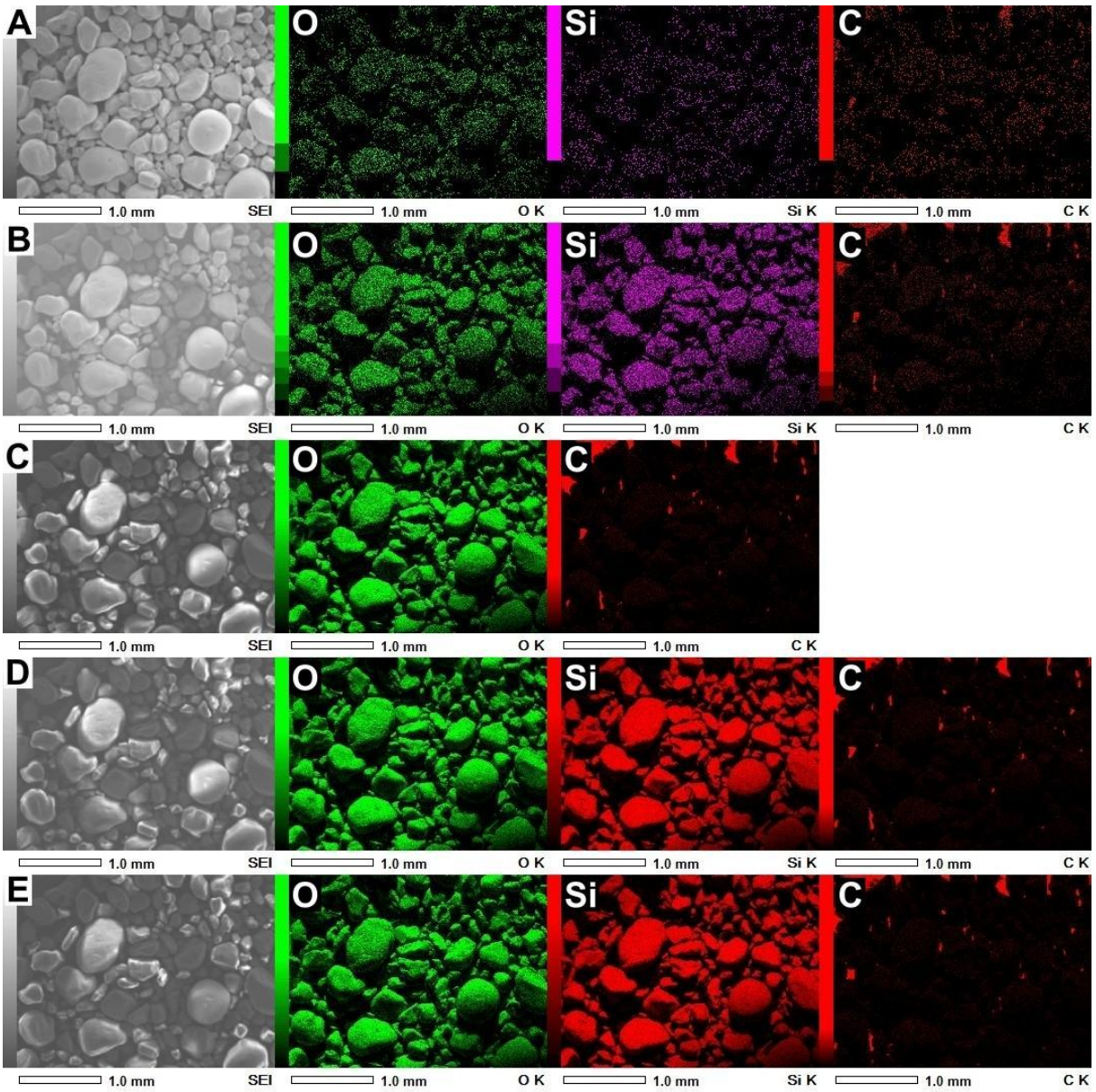

Figure 9. SEM/EDS of coated sand grains (A-E) from 3 to 20keV, respectively. Here, there is no greater detection of elements but there is greater intensity in the elements present as the tension increases. SEI = Secondary Electron Image. Scale bar = 1.0 mm. Spot size = 30 (A-D) and 10 (E). Magnification = x40.

Despite the large amount of data we can obtain through images and maps, spectral comparison (%wt) is also important. For that, we considered values obtained through the sigma, a confidence interval that allows the relative quantification of the elements detected in the sample.

In the case of sand (Figure 10), in general, the best conduction by the electron beam was made in the uncoated sample at tensions between 3 and 10keV (e.g. O, Na, Al, Si, P, S and Ca). Some elements only show presence when the sample is uncoated (e.g. P and S) while others only when the sample is coated (e.g. Ti, Zn and Sr).

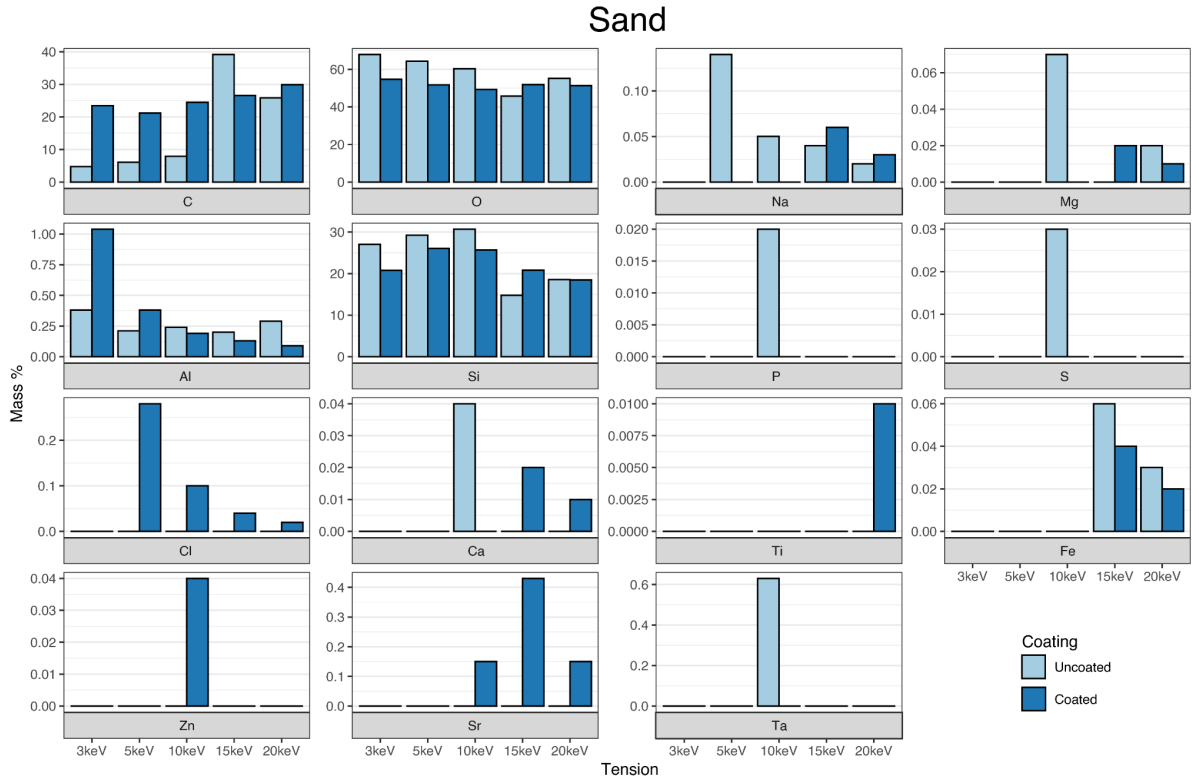

Figure 10. Sand EDS elementary data, separated by coating (coated and uncoated) and by electric tension (x axis - 3 to 20keV). Note that there are elements that only appear when there is uncoated (*e.g.* P and S) and others when there is only coated (*e.g.* Cl, Ti, Zn and Sr). Furthermore, some only appear at certain tensions (*e.g.* P and Ti) and their intensity also differs. The element Ta has been discarded as it is possibly overlapping Si. Created by Gabriel Barros.

At the lowest tensions (3 and 5keV) of the uncoated clay grains, no element was detected as shown in the graphs of Figure 11A. Above these tensions, the elements O, Si, C and Al are detected, with the exception of Mg detected only at 15keV, which can be a specific area where this element is located and/or was more detectable in this tension (Figure 11B). Furthermore, at 15keV we can also observe the elements in higher intensities. In coated clay, on the other hand, it is possible to

see higher intensities of O, C, Si, Al and Mg in the mapping since 10 keV Therefore, high tensions can be more efficient in coated clays (Figure 12).

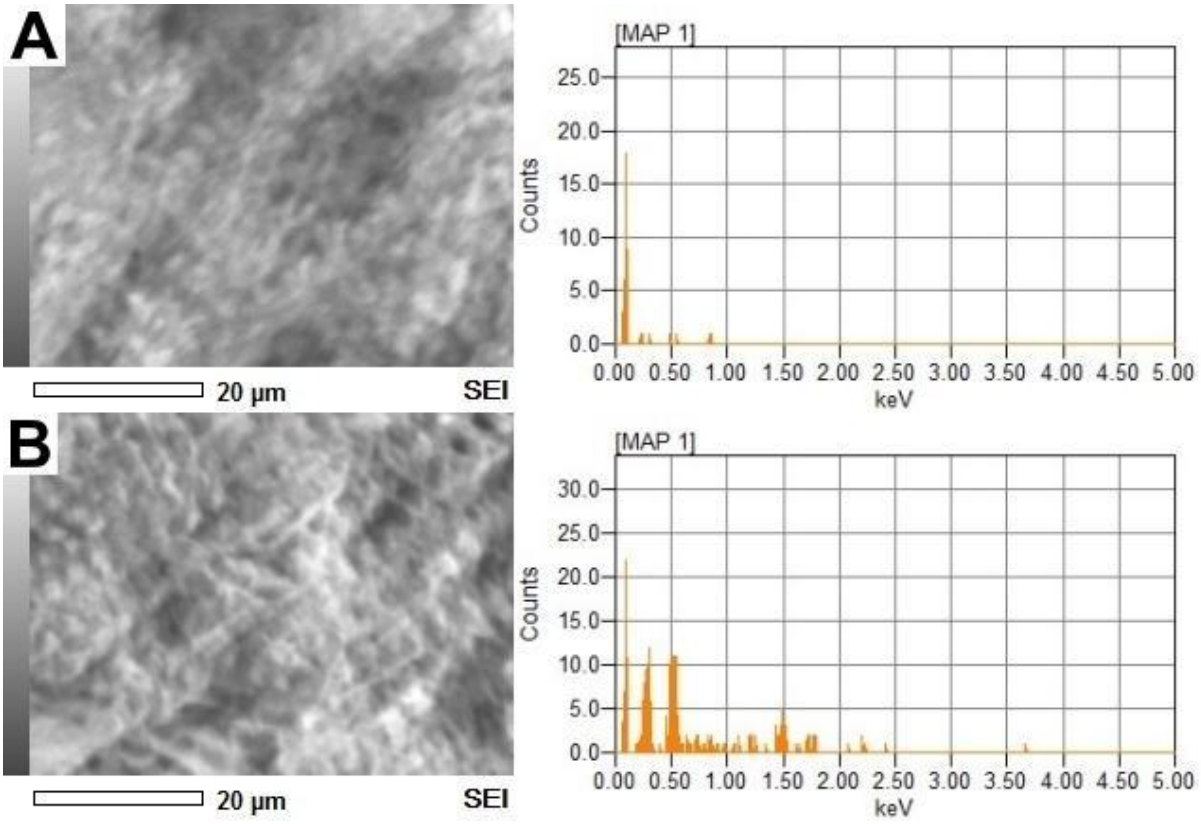

Figure 11A. SEM/EDS of uncoated clay grains in 3 and 5keV (A and B, respectively). Not enough elements were detected to map. SEI = Secondary Electron Image. Scale bar = 20 µm. Spot size = 30. Magnification = x2,200.

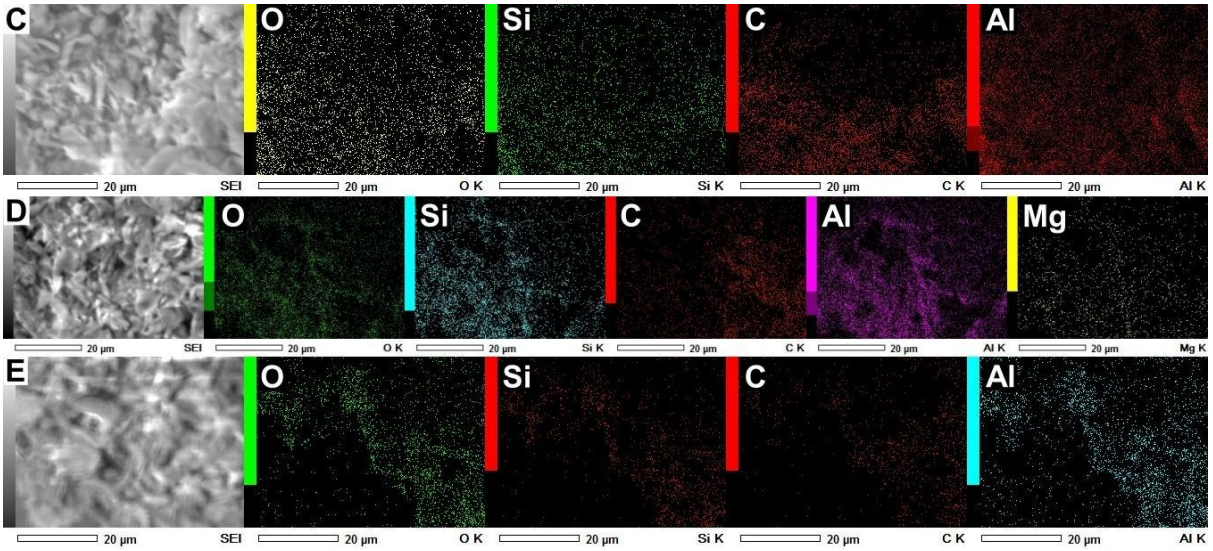

Figure 11B. SEM/EDS of uncoated clay grains in 10, 15 and 20keV (C, D and E, respectively). SEI = Secondary Electron Image. Scale bar = 20 μm. Spot size = 20 (C) and 10 (D-E). Magnification = x2,200.

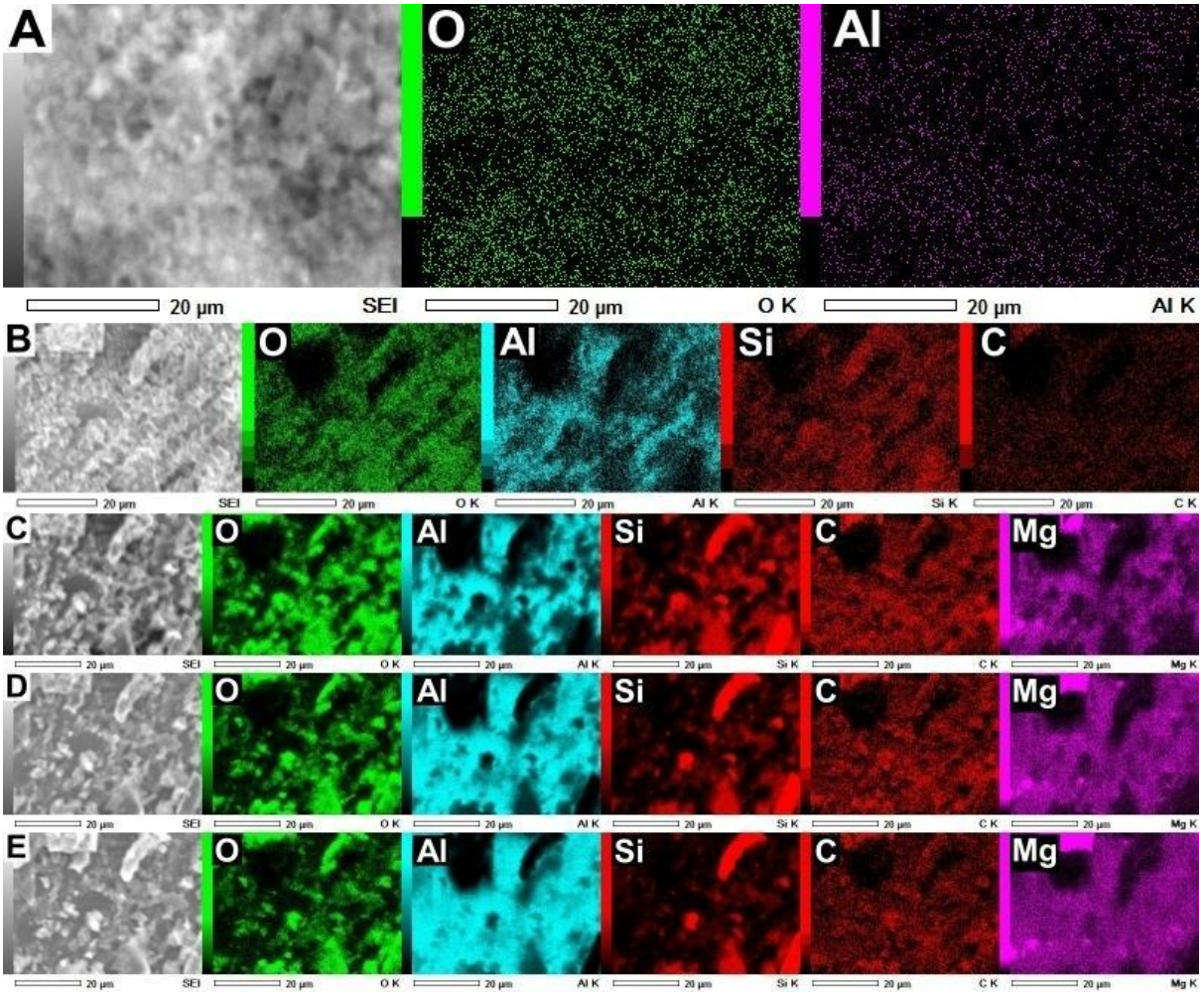

Figure 12. SEM/EDS of coated clay grains at 3 to 20keV (A-E, respectively). SEI = Secondary electron Image. Scale bar = 20 μm. Spot size = 30 (A-C) and 10 (D-E). Magnification = x2,200.

Using the same procedure as the sand grains, the clay also had its sigma analyzed (Figure 13). As a result, we observe that, unlike sand, most elements are detected when the sample is coated and some elements as Cl, Ca, Mn and Sr are only detected in this situation. Anyway, in the case of clay, the “optimal tension” varies between 5, 10 and 15keV.

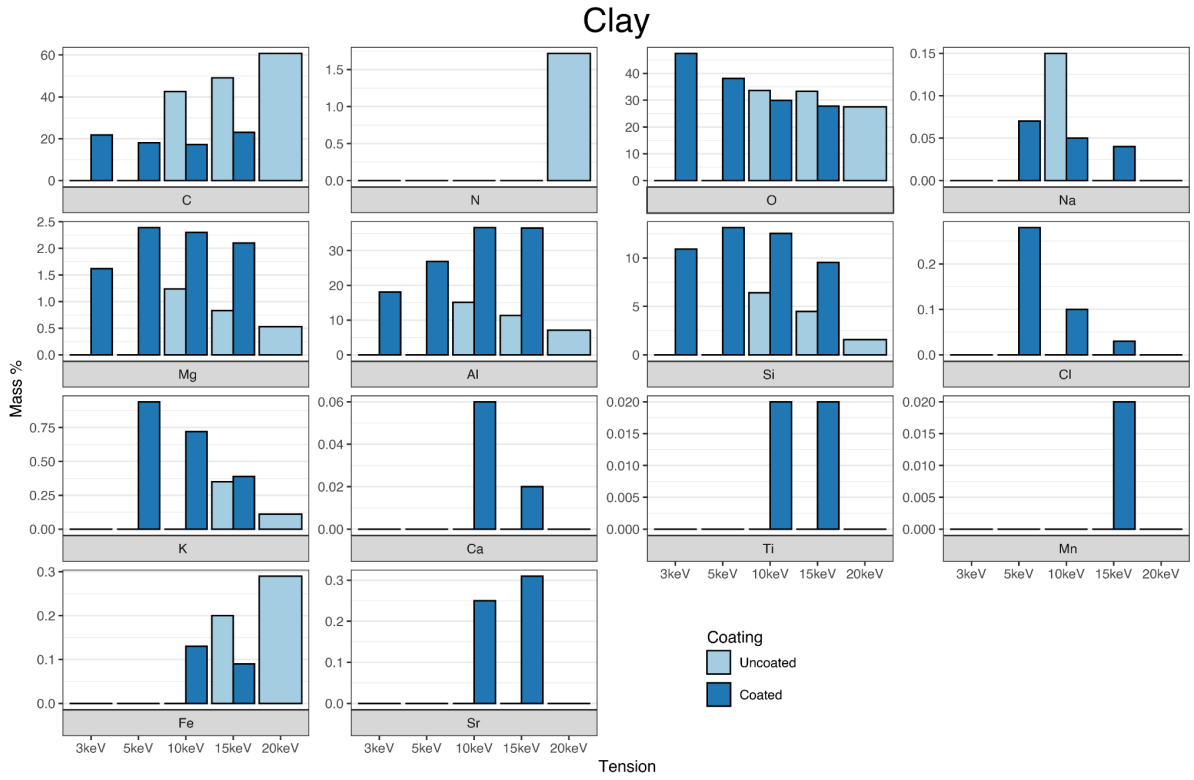

Figure 13. Clay EDS elementary data, separated by coating (coated and uncoated) and by electric tension (x axis - 3 to 20keV). As for sand, we can also observe some elements that only appear at certain tensions (*e.g.* Cl, Ca, Ti, Mn and Sr) as well as at certain intensities. No data from coated 20keV samples. Element N was discarded for being considered contamination. Created by Gabriel Barros.

The rock matrix (sediments) from samples of Lontras Shale were also analyzed by EDS. In this case, we have the sedimentary and organic heterogeneity of a shale (Figure 14).

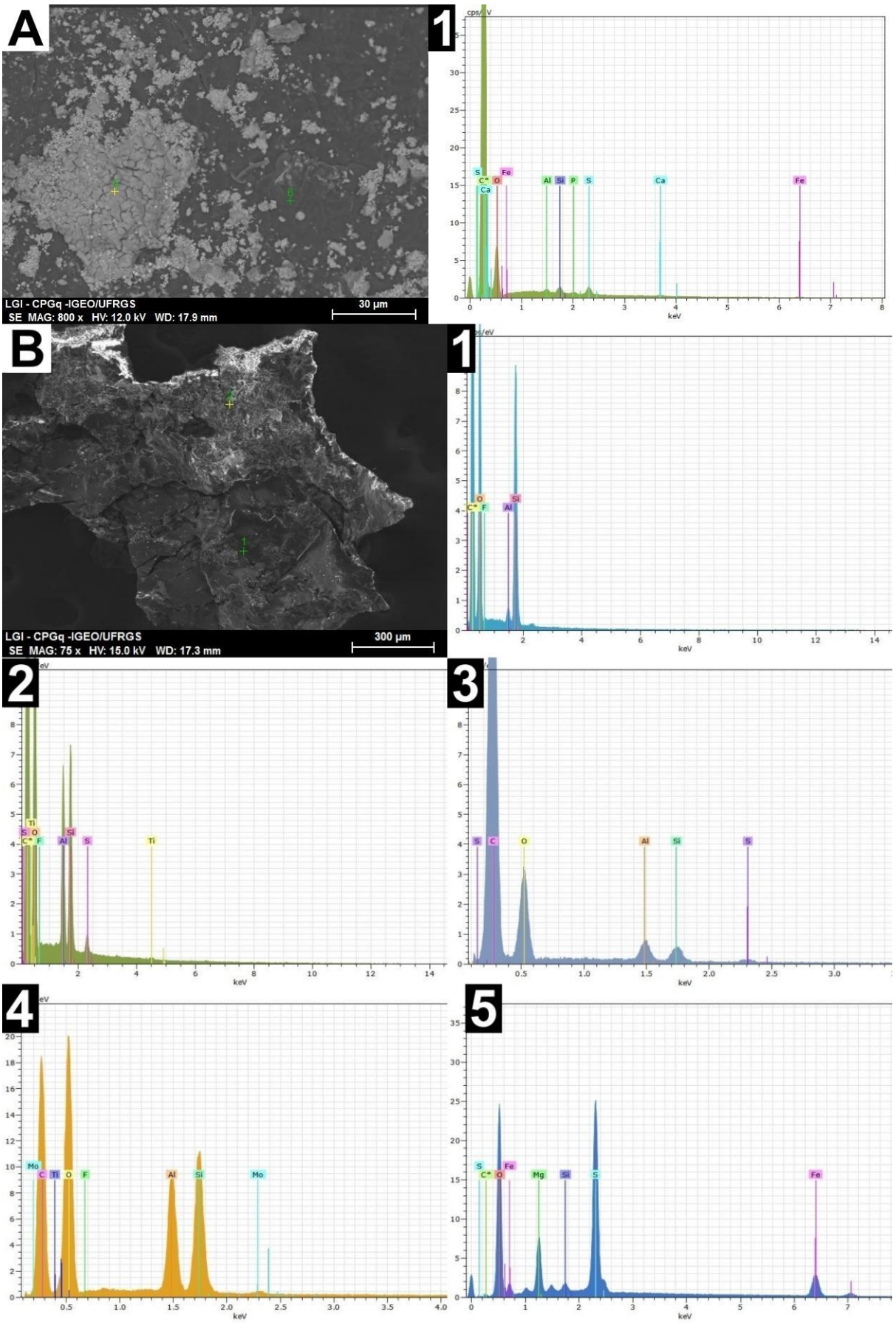
A
1
LGI - CPGq -IGEO/UFRGS
SE MAG: 800 x HV: 12.0 kV WD: 17.9 mm
30 µm
B
1
LGI - CPGq -IGEO/UFRGS
SE MAG: 75 x HV: 15.0 kV WD: 17.3 mm
300 µm
2
3
4
5
keV

Figure 14. EDS plots of the sediment of the Lontras Shale at 12 and 15keV, respectively. In these graphs, it is possible to observe the variety of elements that is composed *in situ* sediment. Magnification = 800x (A) and 75x (B). Scale bar = 30 μm (A) and 300 μm (B).

4.2.2. Fossil

As mentioned before, fossils are heterogeneous materials usually composed by several minerals, so a wide variety of elements can be found in them. In the case of coated lycopsids fragments we can observe that between 3 and 10keV (Figure 15) the electron beam can detect a reduced number of elements when compared to the 15keV mapping (Figure 16). Also, with the increase in tension and consequent greater penetration of electrons, we detected both more superficial elements as well as trace elements, including Rare-Earth Elements (REE), such as Y.

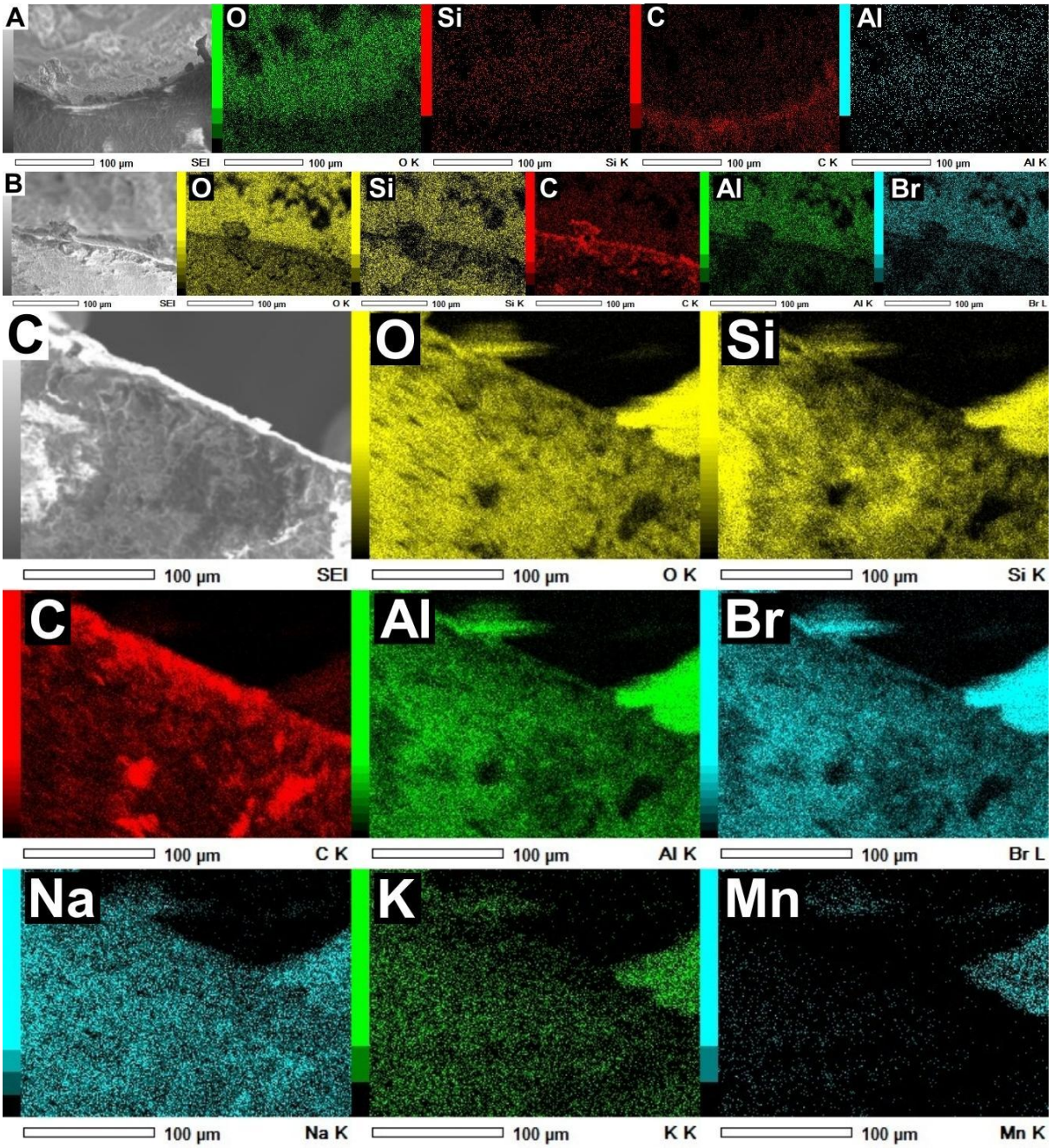

Figure 15. EDS maps of the fossil stem fragment at 3, 5 and 10keV with spot size 70 (A-C, respectively). Here we can observe that with the gradual increase in tension, the elements O, Si, C and Al are shown to be more intensified, and other elements are also detected. SEI = Secondary Electron Image. Scale bar = 100 µm.

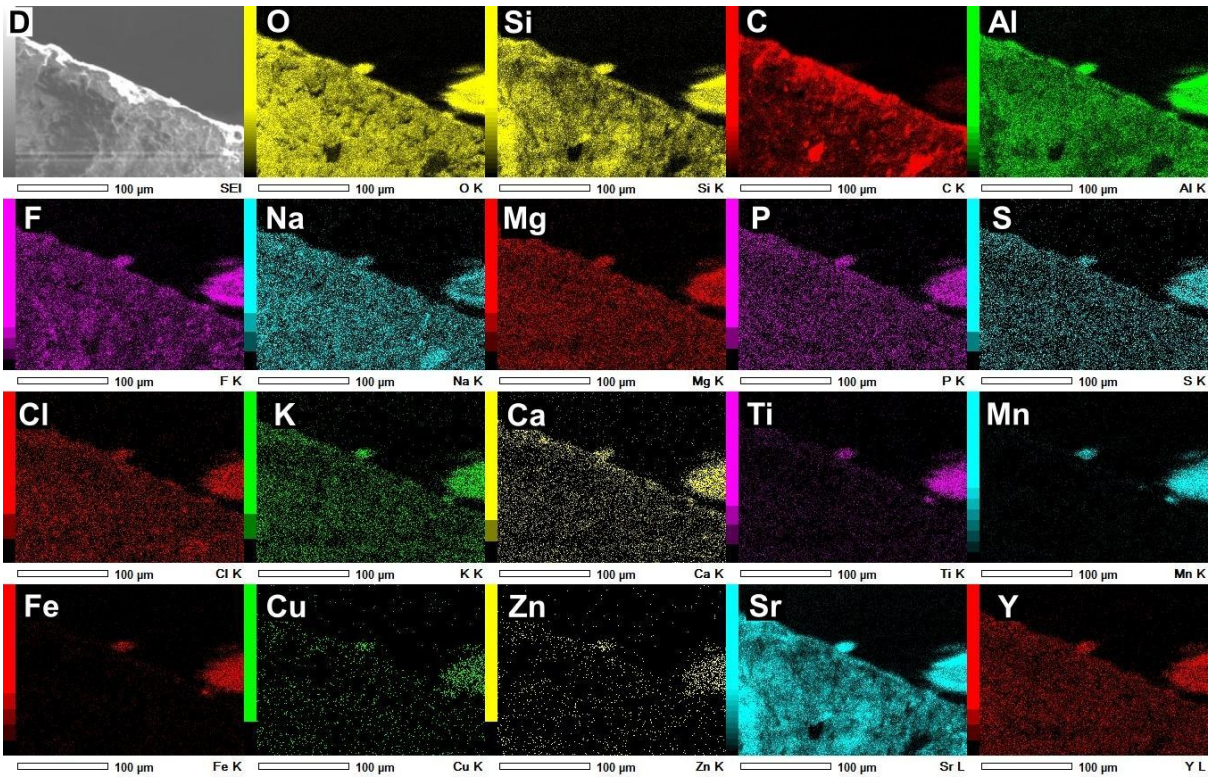

Figure 16. EDS maps of the stem fragment at 15keV, spot size 70. In these maps we can see how this tension manages to detect a wide variety of elements, from lighter to heavier ones. SEI = Secondary Electron Image. Scale bar = 100 µm.

In addition to varying the tensions, we also varied the spot size and magnification at the 15keV mappings. In the case of spot size, we changed it to 30 (Figure 17) without major changes other than not detecting Zn. In the case of magnification, when we increase it to 2700 (Figure 18), we can see a reduction in the detection of elements. At the same time, we observed more heterogeneity of intensities in higher magnifications: in the possible EPS region we detected higher intensities of Al, C and Fe in comparison to other parts of the fossil; and some combinations of Na and C as well.

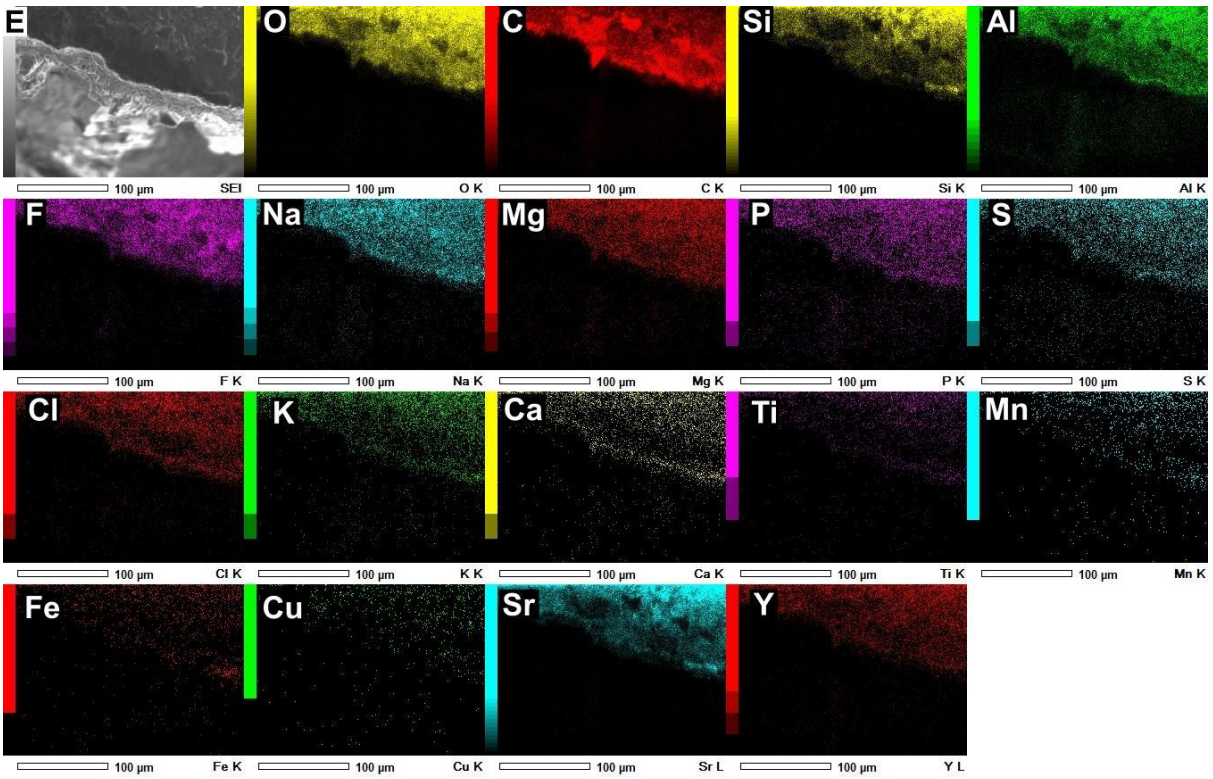

Figure 17. EDS maps of the stem fragment at 15keV, spot size 30. As in the previous figure, we can observe several elements minus Zn. If there is a specific interest in this element, it might be important to be careful with the spot size. SEI = Secondary Electron Image. Scale bar = 100 µm.

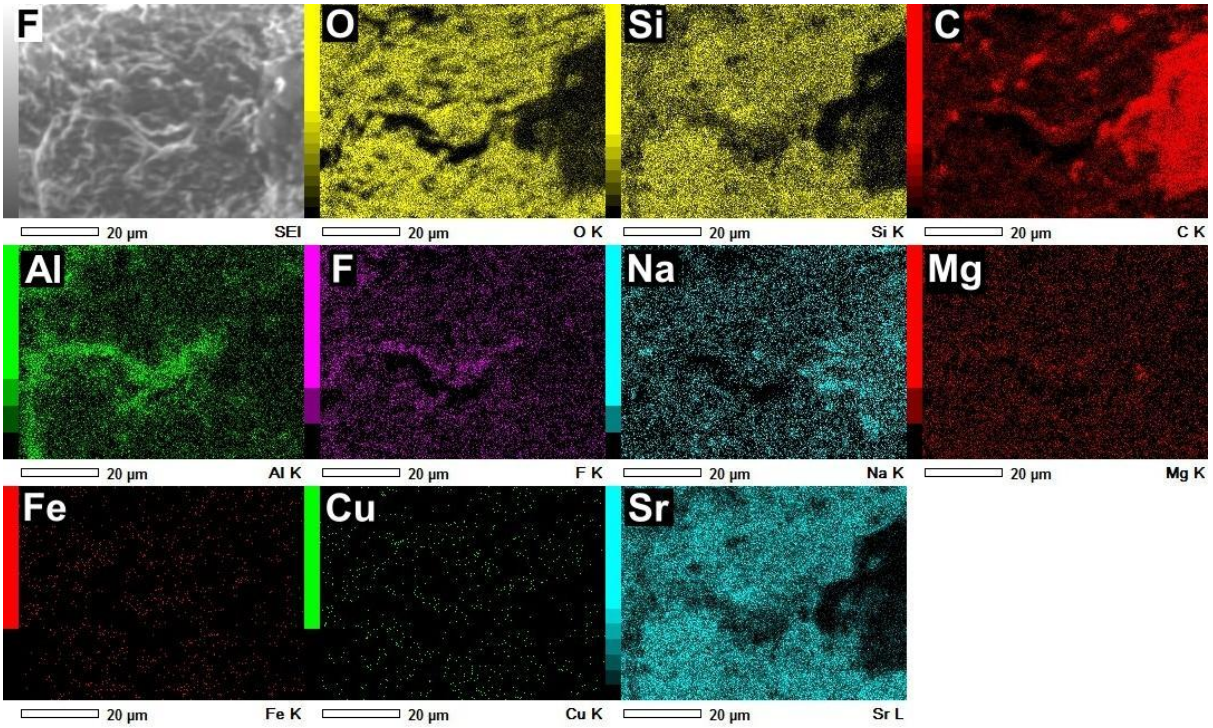

Figure 18. EDS maps of the stem fragment at 15keV, spot size 30, magnification x2700. Here we can see a reduction in the amount of elements detected. SEI = Secondary Electron Image. Scale bar = 20 µm.

As well as we perform in sediments, we also plot the sigma graphs of the stem fragment (Figure 19), where we can observe that the great heterogeneity of this type of sample also implies element detection. Therefore, the ideal is to have an idea of what you are looking for as some elements are more restricted to some tensions (e.g. Zn, Br and Y), while others are more comprehensive (e.g. Si, C, O and Al).

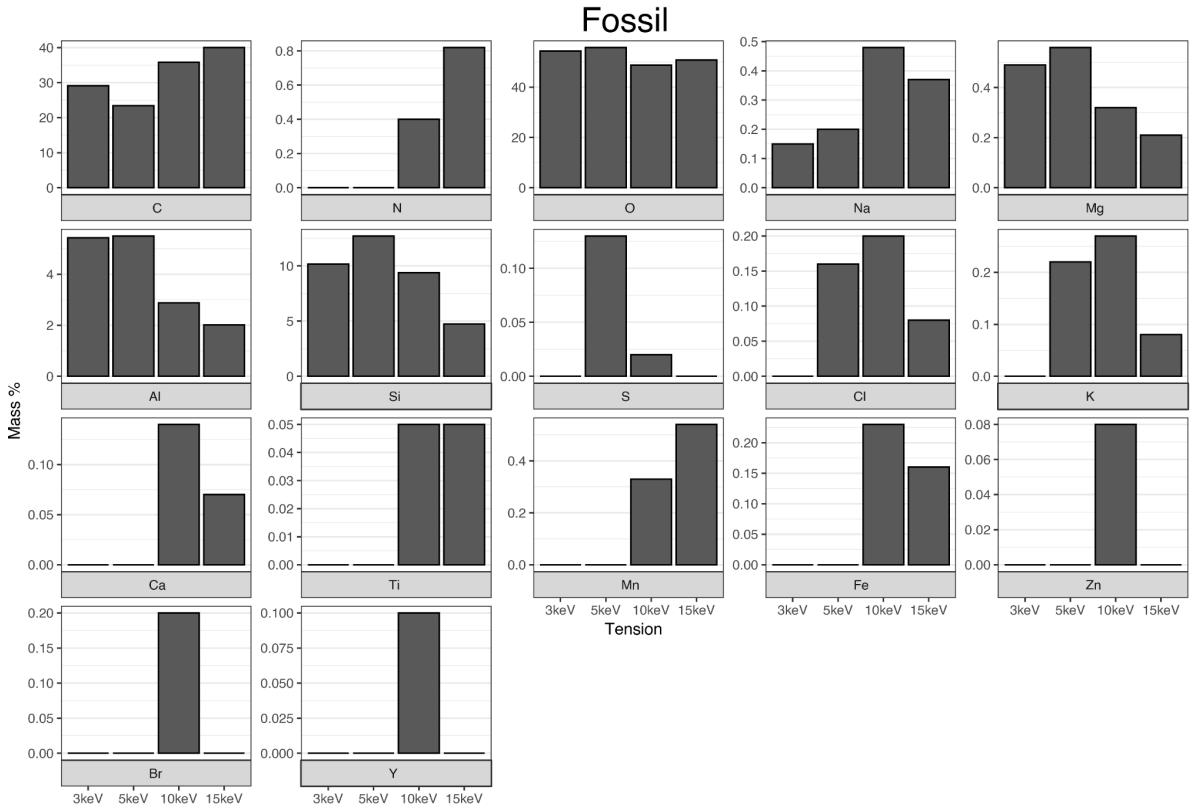

Figure 19. EDS elementary data of the stem fragment. Note how some elements are more encompassing between tensions (e.g. C, O, Na, Mg, Al and Si) while others are more restricted to specific ones (e.g. Zn, Br and Y). Here we also indicate element N as sample contamination. Tensions: (x axis - 3 to 15keV). Created by Gabriel Barros.

The EDS maps of the muscle from Lontras Shale insect were also made using 3 to 20keV tensions (Figure 20a, b, c). We observed in the insect's muscle that the increase in tension detects more elements, including elements that can be considered trace elements (e.g. Na and Ti).

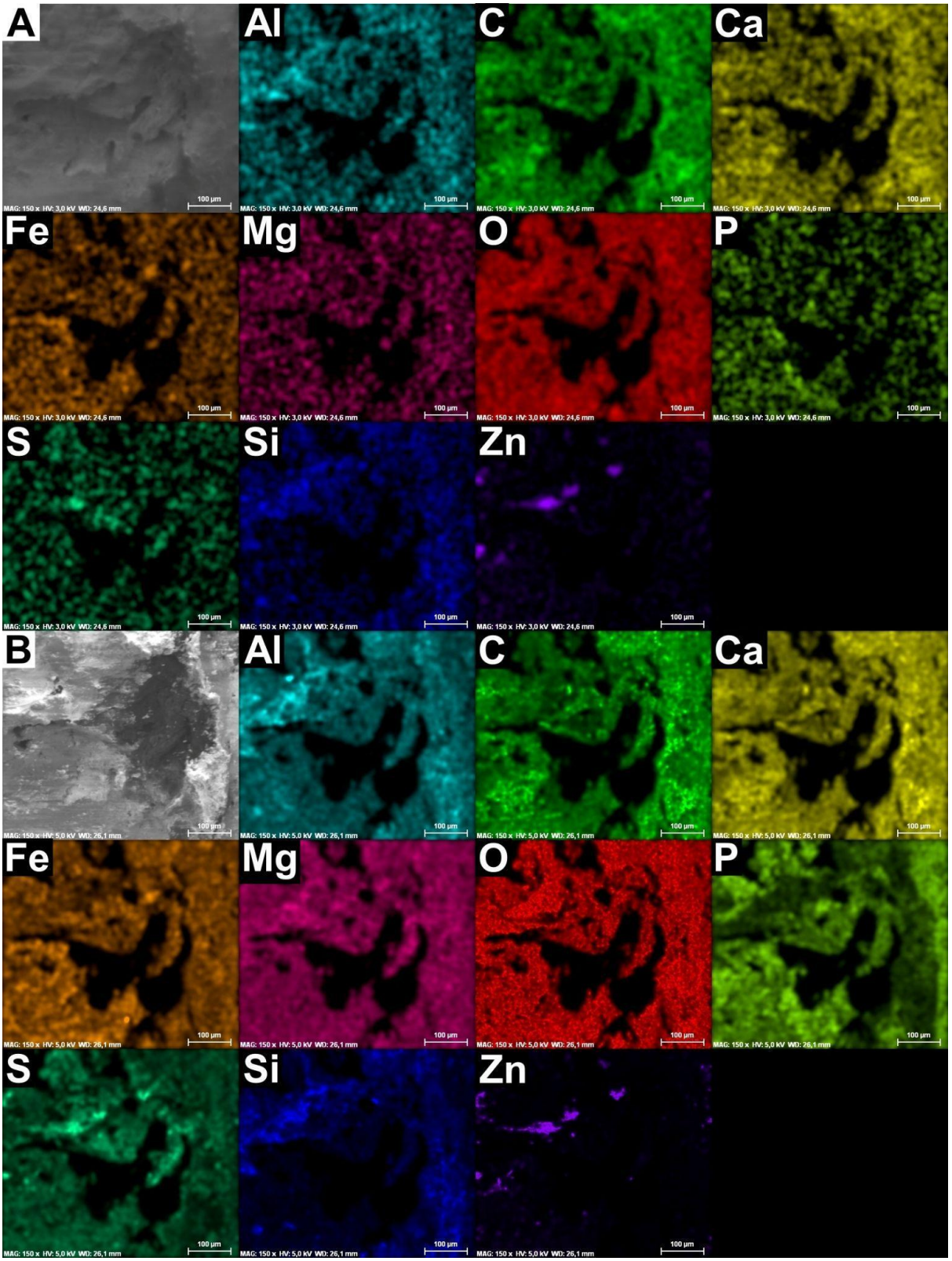

Figure 20a. EDS maps of the insect's muscle from Lontras Shale insect at 3 and 5keV (A and B, respectively). Here, the two tensions show the same amount of elements, which may mean that these elements are on the surface. Magnification = x150. Scale bar = 100 µm.

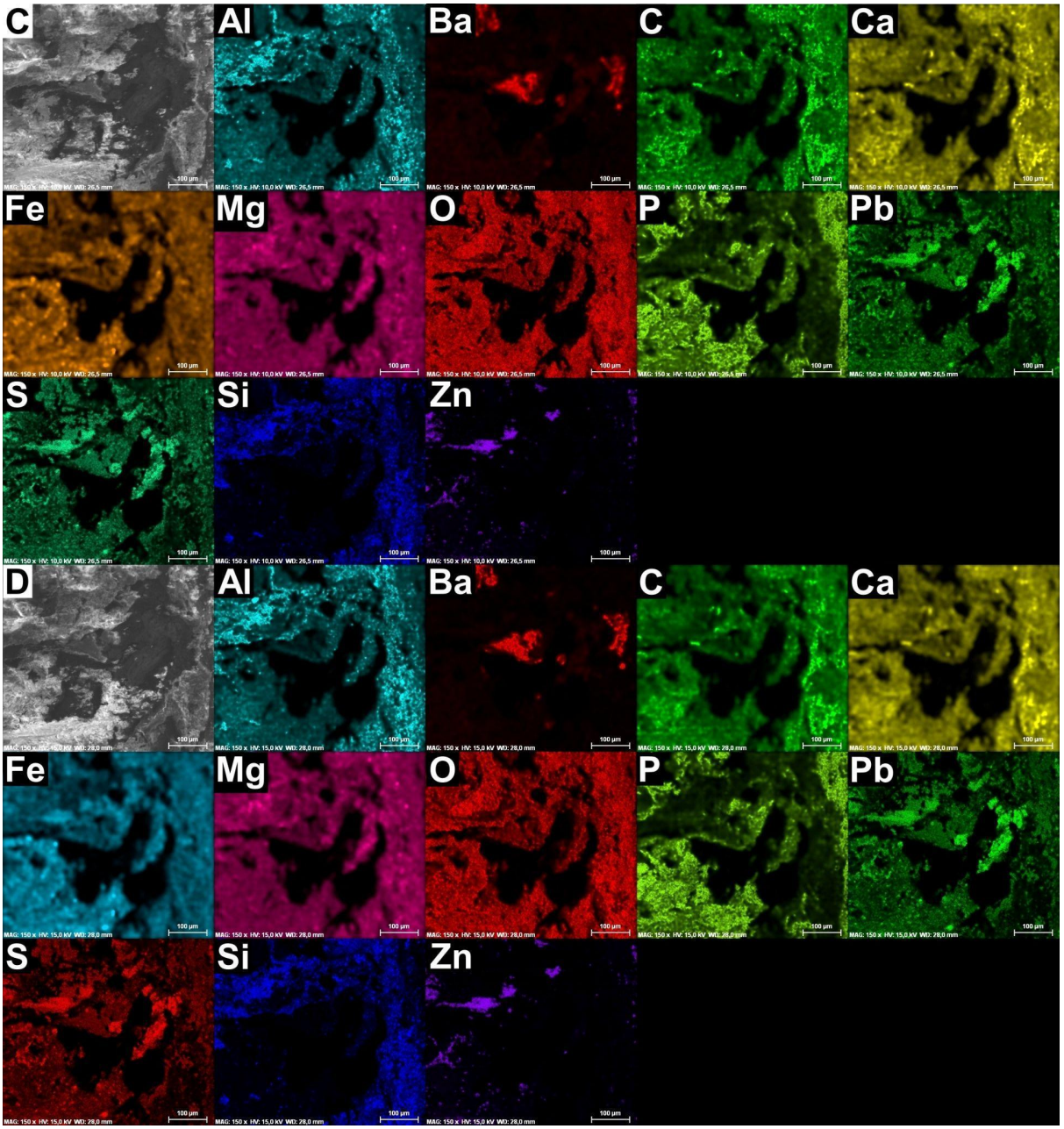

Figure 20b. EDS maps of the insetct's muscle from Lontras Shale insect at 10 and 15keV (C and D, respectively). Note the presence of Ba and Pb increasing the number of elements and the laser depth. Magnification = x150. Scale bar = 100 µm.

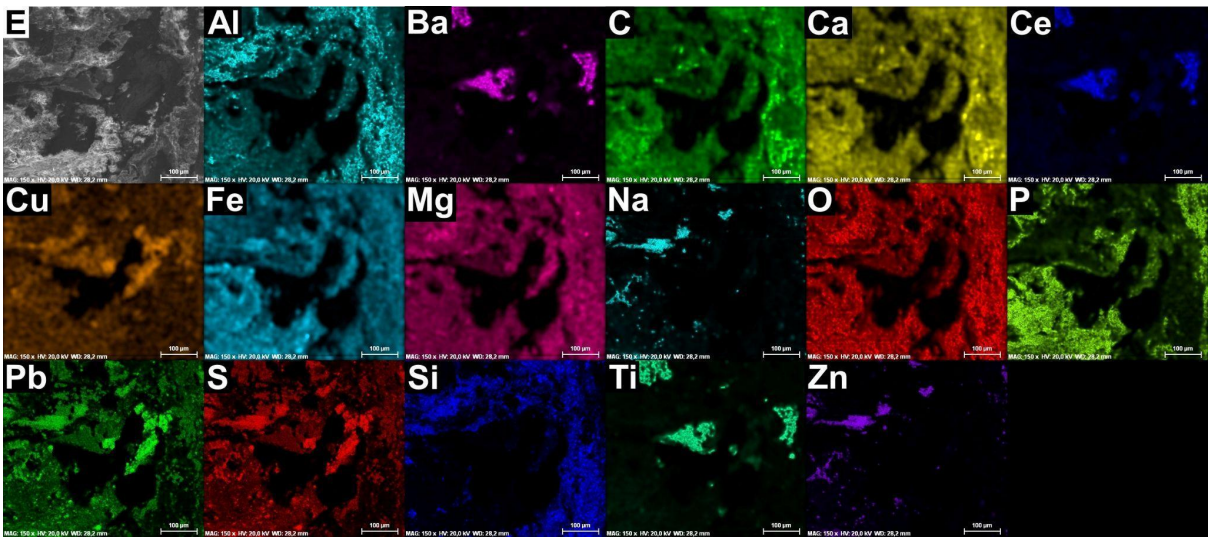

Figure 20c. EDS maps of the Lontras Shale insect's muscle at 20keV. In addition to all the elements already observed in other tensions, here also appear elements that may be more related to a deeper region of the sample, which may characterize them as trace elements (e.g. Ce, Cu, Na and Ti). Magnification = x150. Scale bar = 100 µm.

As we can see, as the tension used is increased, that is, the electron beam penetrates more into the sample, more elements can be detected. Some of these elements can be found as trace elements, some of which we can also observe in the µXRF analysis (Figure 21).

µXRF detected the presence of some elements seen in EDS: Ca, Fe, Mn, Si and Ti. Although Si is considered a lighter element, due to its large quantity, it also appears in µXRF. In addition to all this, µXRF also detected the heavy elements Cu, P, Sc and Zn.

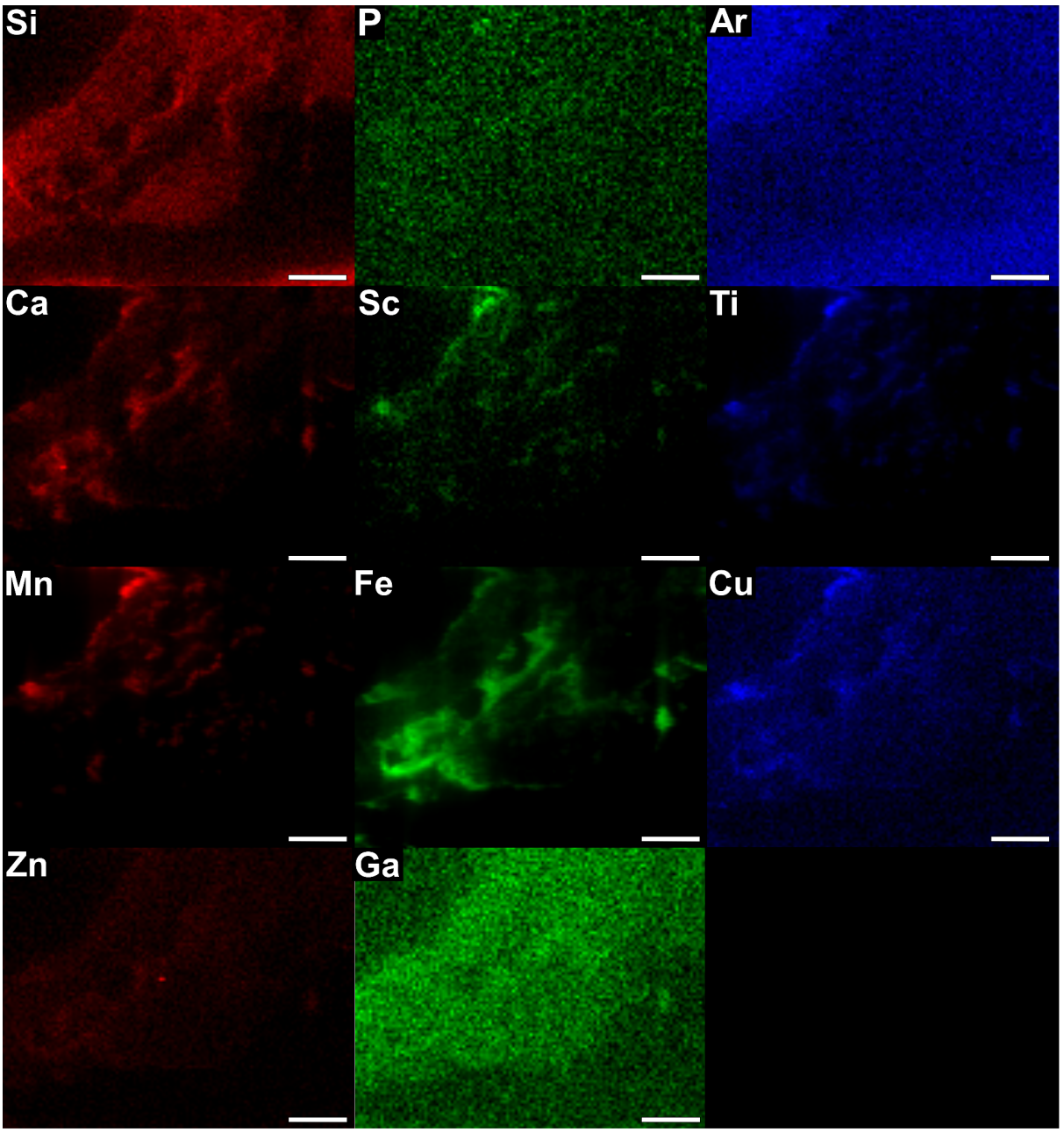

Figure 19. μXRF maps of the stem fragment. As in the EDS, the heterogeneity of the sample is present in the mapping of elements that, in the majority, were present in the EDS but detected with low intensity. Here, as it is a more delicate technique, we can observe these elements more specifically. Scale bar = 20 mm.

In terms of element mapping, we can observe that the EDS and μXRF techniques, when used in a complementary way, can maximize the analysis, seeking

not only to map the superficial and deep elements, but also light and heavy elements. In the case of EDS both and, for μXRF, mostly heavy elements.

4.3. Cathodoluminescence (CL)

The analyzed sediments included moderately-sorted, angular to subrounded quartz sand grains in fine to medium fractions, which exhibited homogeneous luminescence signatures, in shades of dark to light blue. Light shades occur mainly along with irregularities in the grain edges and in iron oxide films that partially cover some grains. Scattered luminescent spots on the grains and along the impregnating resin of the blades show a phosphorescent green to deep red color. As for the textural aspects, the quartz grains present abrasion edges, percussion marks, dissolution marks, and drag streaks.

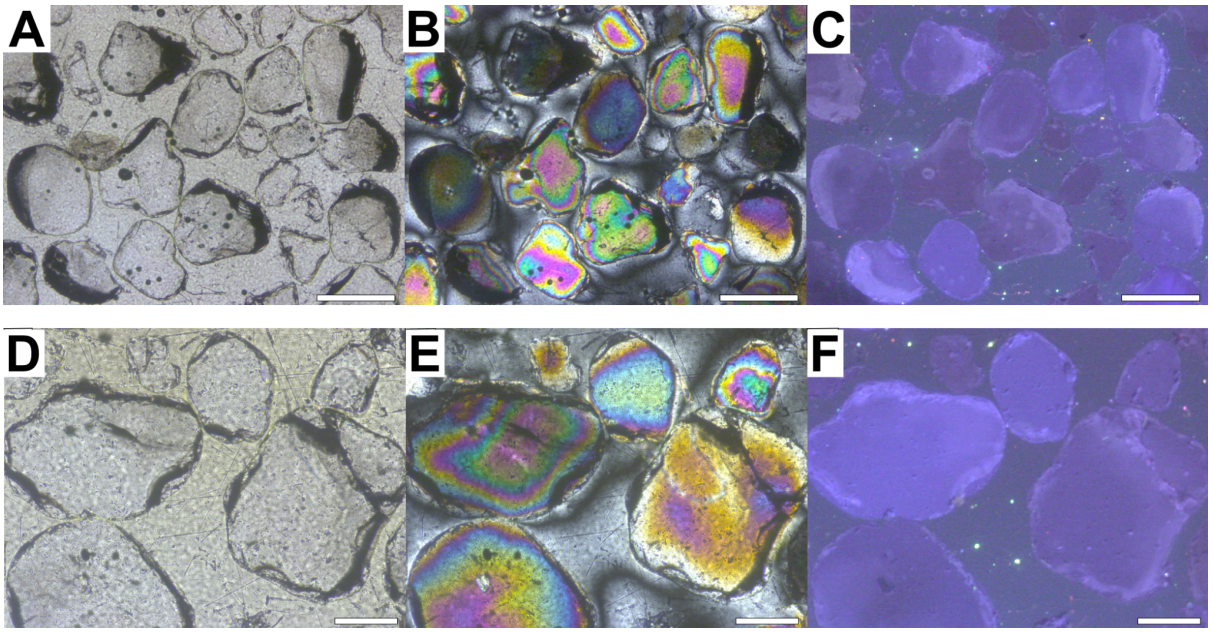

Figure 22. CL of sand. Note iron films alongs grain boundaries in Fig. A and irregularities in the grain edges in Fig. D. Cathodoluminescence analysis revealed homogeneous blue signatures in quartz grains. A and D = Natural light; B and E = Crossed nicols; C and F = CL. Scale bars: A-C = 500μm; D-F = 200μm.

4.4. Micro-Raman Spectroscopy (μRaman) and X-Ray-Diffranction (XRD)

4.4.1. μRaman

4.4.1.1. Sediments

Analyzes in μRaman were performed with samples of pure sediment (sand and clay), lycopsid stem fragment and data obtained from the Lontras Shale (Mouro et al., 2020). The first graph (Figure 23) presents the μRaman spectrum of sand (quartz) analyzed by two different lasers: 532 and 785 nm. Visually, we can see the characteristic quartz peak close to 500 cm-1 in both lasers. However, the 785 nm laser stands out for its greater capacity for detecting quartz minerals.

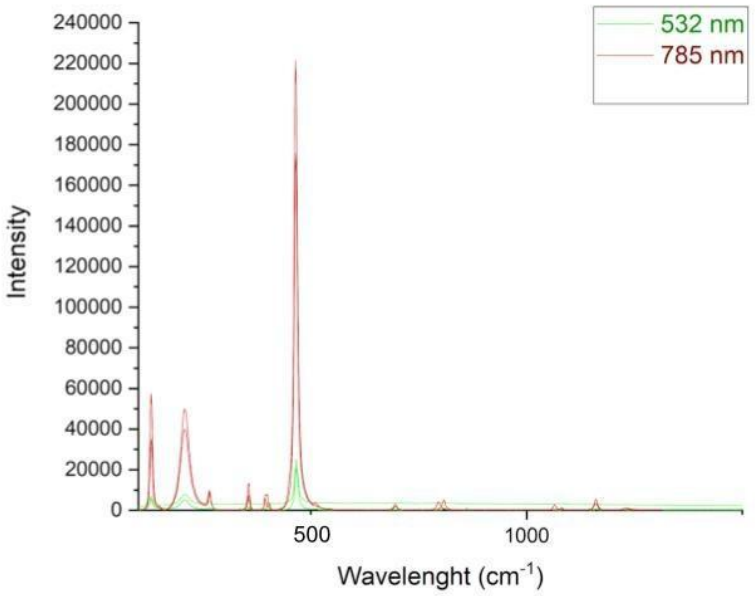

Figure 23. μRaman spectra of sand quartz with different lasers: 532 (green peaks) and 785 nm (red peaks). Observe higher intensities of quartz peaks at 785 nm.

The μRaman spectrum at center 750 (Figure 24-A) shows that there is great similarity in composition among the 30 samples, with emphasis on quartz peaks at 129, 207 and 465 cm-1. In addition, we can observe that some specific samples present shifted peaks. In comparison, the spectrum at center 1800 (Figure 24-B) has intense noise, some shifted peaks and amorphous carbon (1356 cm-1) (organic contamination?).

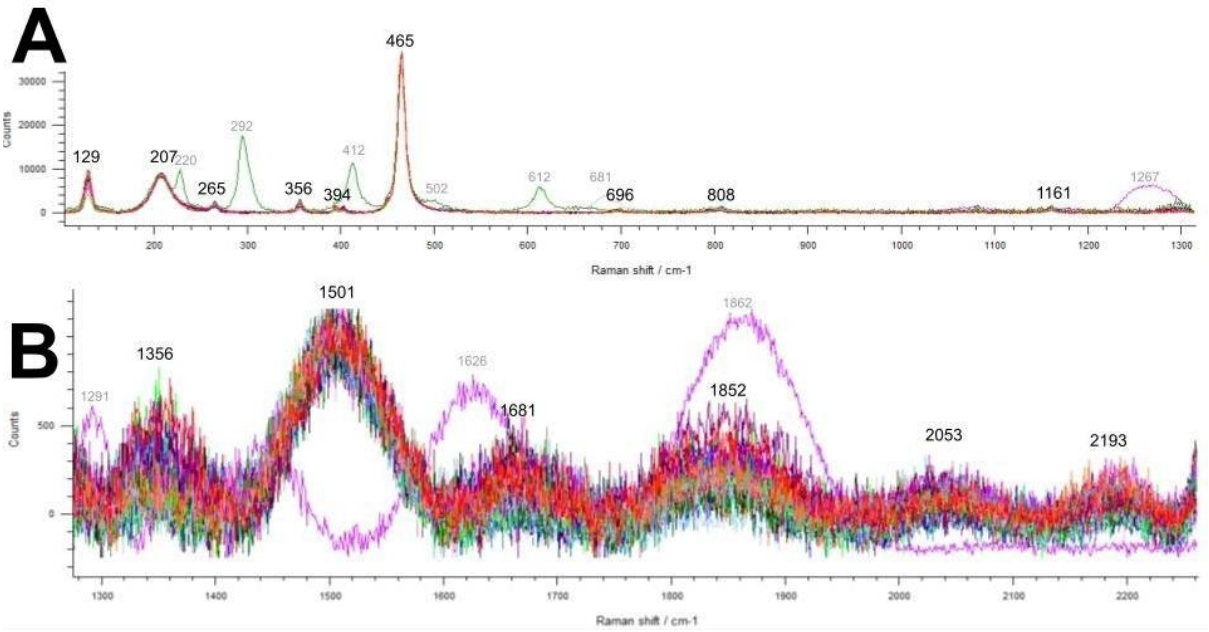

Figure 24. µRaman spectra of sand quartz (n=30) with 785 nm laser and 750 center (A) and 1800 center (B). Peaks highlighted in black are common to all samples. The gray peaks are specific to some samples.

At the spectrum of illite clay it is possible to observe peaks related to quartz (129 cm-1), anatase (195 and 637 cm-1) and calcite (707 cm-1) (Figure 25-A). To show how much diversity there can be, even in the same sediment, we plotted a graph with 30 spectra from different points on the illite, where we can see that the sediment shares several components in common but varies in peak intensity (Figure 25-B).

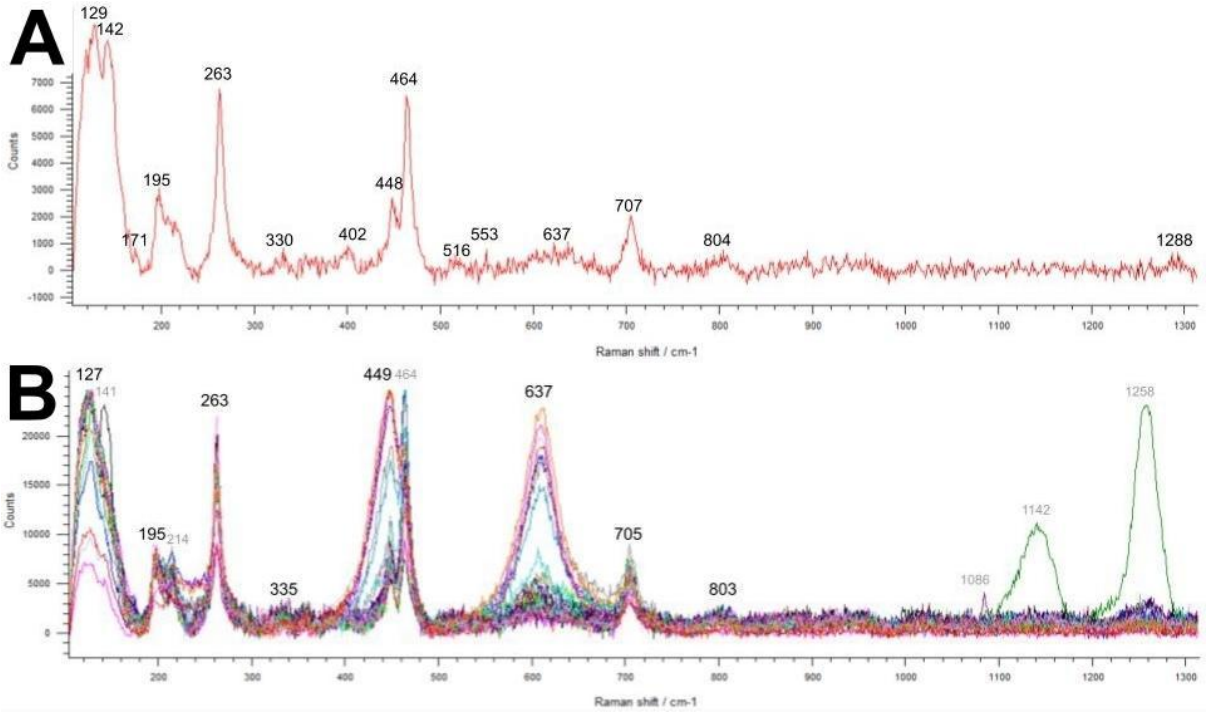

Figure 25. µRaman spectra of clay illite (A) and (B) with 785 nm laser and 750 center. Peaks highlighted in black are common to all samples. The gray peaks are specific to some samples. N=30.

4.4.1.2. Fossils

In the spectrum of the silicified lycophyte fragment (Figure 26), three points were selected for analysis. In this case, it is possible to observe how the points share peaks in common, allowing the observation of anhydrite? (119 cm-1), calcite? (153, 282, 712 and 1086 cm-1), and quartz (212 cm-1; 465 cm-1).

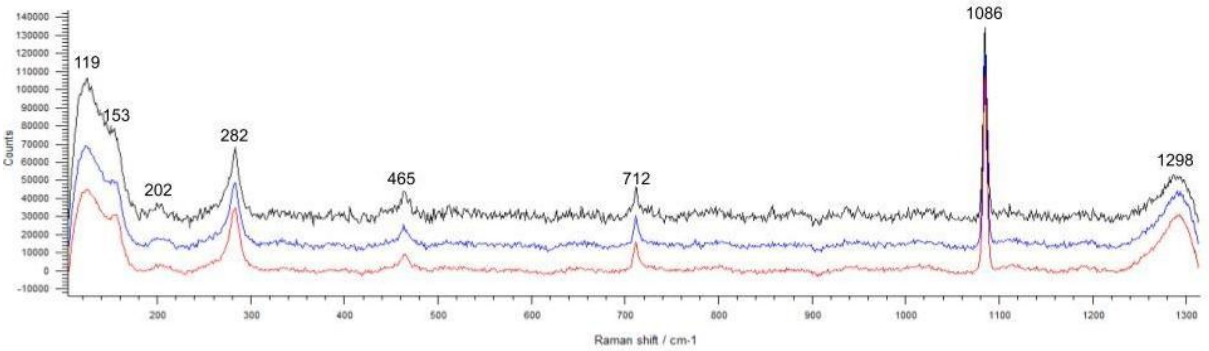

Figure 26. µRaman spectra lycopsid stem fragment number 1 with 785 nm laser and 750 center.

Considering this heterogeneity of the fossils, we analyzed the external part of the lycophyte fragment (bark) and the internal part (core). The bark (Figure 27-A) showed a more homogeneous composition with anhydrite? (120 cm-1), and quartz (202 cm-1; 464 cm-1). The core of center 750 (Figure 27-B), has some subtle differences between the analyzed points, although they also share, in general, the same peaks. In addition, the quartz peaks present in the core are more intense than the bark peaks.

The core at center 1800 was also analyzed (Figure 27-C) which, as in the sand, shows very intense noises.

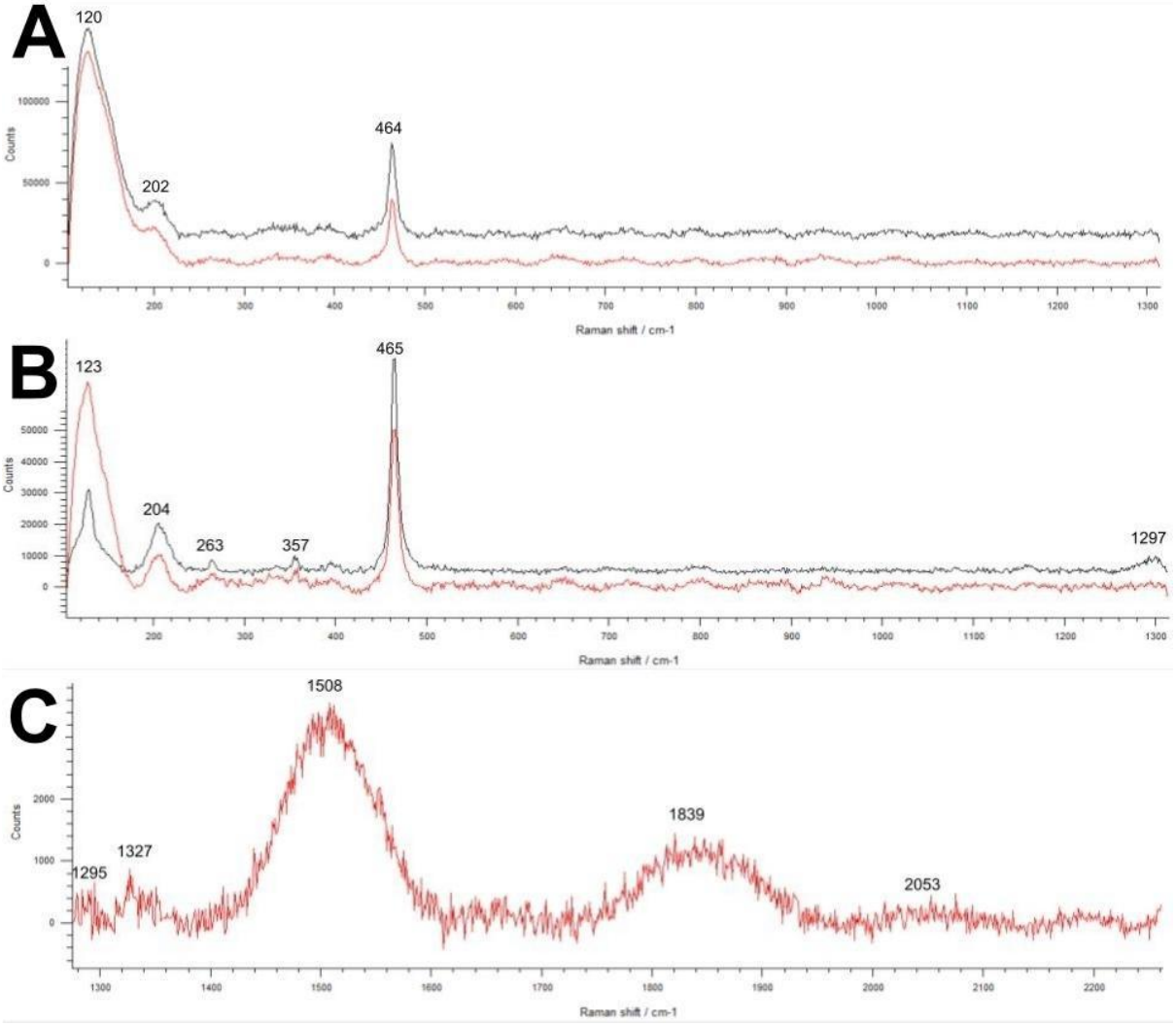

Figure 27. μRaman spectra from the bark (A) and the core (B) of lycopsid stem fragment number 2 with 785 nm laser and 750 center and the core in 1800 center (C).

Figures 28A and B show several random points analyzed in the same lycophyte fragment. Here, we can observe the diversity of information about the minerals that the same sample can carry depending on the area observed, even though they share common peaks such as quart in lesser or greater intensity. Based on the spectra, we were able to observe anatase (398 cm-1), quartz (464/465 cm-1), albite (652 cm-1) and probably dolomite? (723 cm-1) peaks.

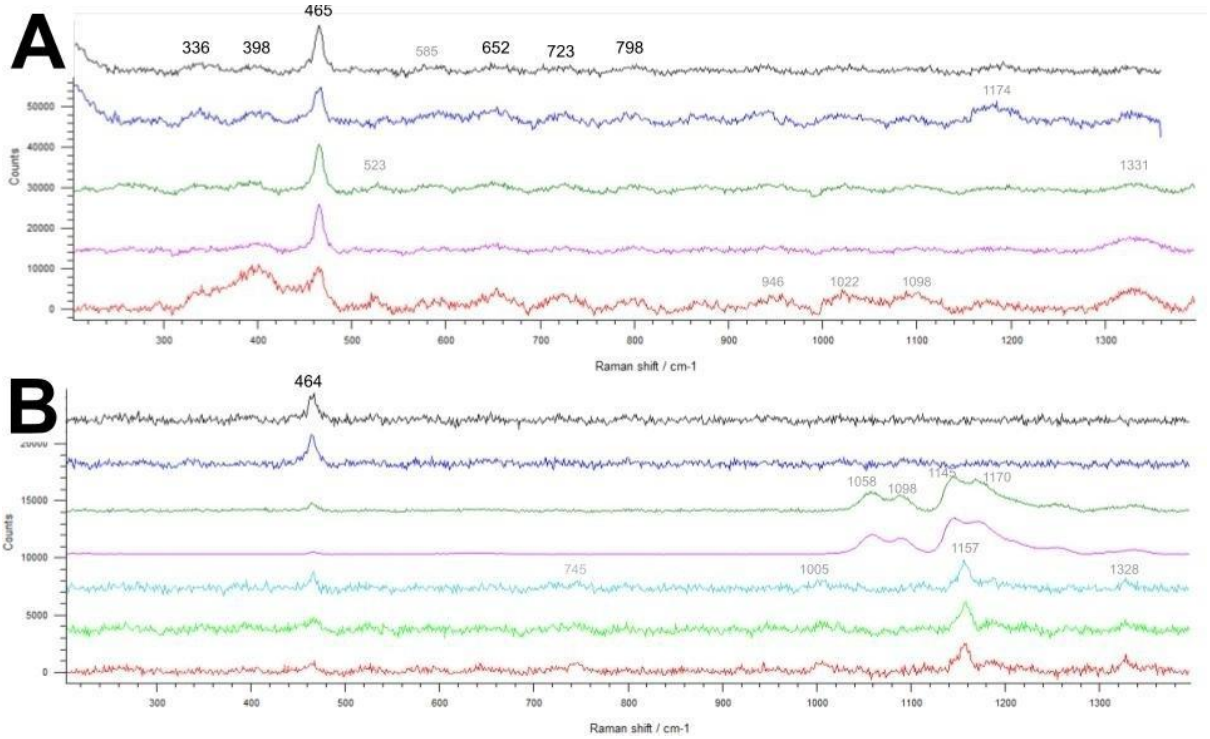

Figure 28. μRaman spectra of lycopsid stem fragment number 3 with 785 nm laser and 750 center. Peaks highlighted in black are common to all samples. The gray peaks are specific to some samples.

Finally, μRaman analyzes were performed considering the Lontras Shale insects. The analysis between wing and matrix detected anhydrite (1178 cm-1) (Figure 29-A) and wing and membrane also detected anhydrite (1016 cm-1) (Figure 29-B). In the case of the wing and rib (Figure 29-C), the spectra are more homogeneous with the peak of amorphous carbon at 1343 cm-1 highlighted. As in the analysis of the bark and core of the lycophyte stem fragment, it was possible to

observe in the different parts of the insect's wing how the characterization of these minerals behaves.

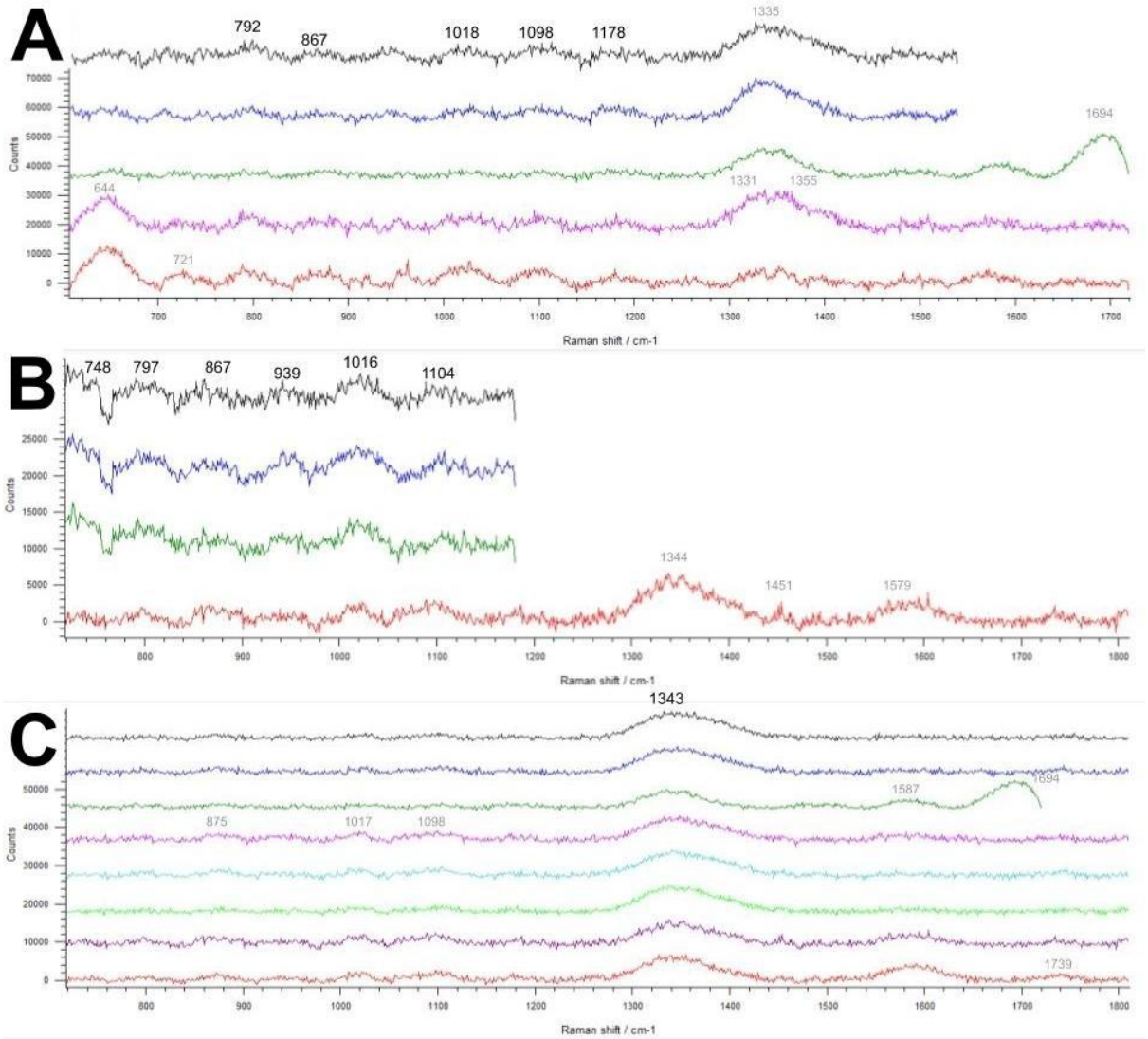

Figure 29. μRaman spectra of insect wing/matrix (A), wing/membrane (B) and wing/rib (C) from Lontras Shale with 785 nm laser. Peaks highlighted in black are common to all samples. The gray peaks are specific to some samples.

4.4.2. X-Ray-Diffraction (XRD)

In this section, we analyze the x-ray diffraction of sand and clay. In the case of sand, minerals of the feldspar family associated with sand were identified (Figure 28). In clay, aluminosilicate hydroxides (pyrophyllite) and aluminum oxide hydroxides (diaspora) were identified, as well as quartz associated with illite (Figure 31).

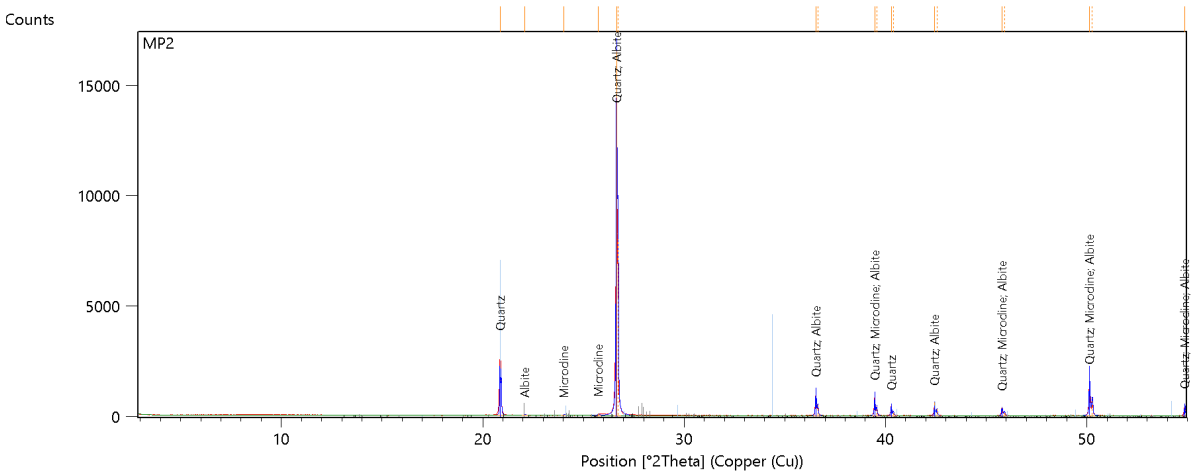

Figure 30. Sand sample diffractogram. Detection of quartz with some albite and microcline.

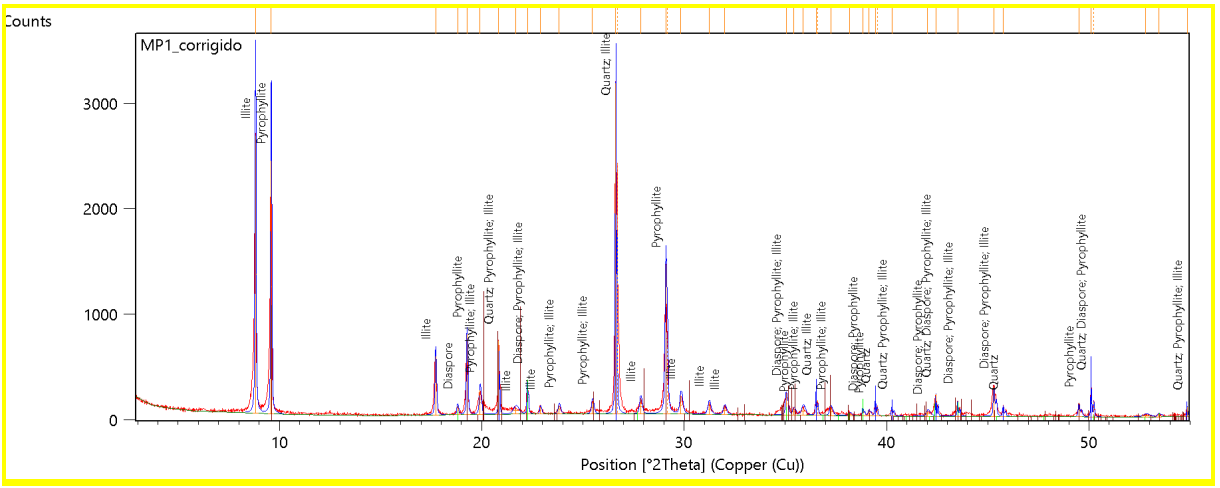

Figure 31. Clay sample diffractogram. Detection of illite with some pyrophyllite, diaspore and quartz.

5. Discussion

5.1. Scanning Electron Microscope (SEM)

5.1.1. Sediment

In the sediments analyzed here (sand and clay) we observed that when uncoated and under low tensions, it is possible to observe the surface details of the grains (especially in sands) and, when coated under low or high tensions, it is possible to better recognize the depth and some additional surface characteristics. The sediment composing the shale rock matrix of Lontras Shale seems to follow the

same pattern. In the case of the silicified lycopsid fragments, we understand that the minerals filling the stem can be comparable to sands (quartz).

The study of sand grains (comparable to quartz and subsequent phases in fossil, rocks and sediments) under SEM may help to reveal different depositional environments, by the recognition of features as as micro-textures, roundness and other surface details (Krinsley and Margolis, 1968; Kleesment, 2009; Vos et al., 2014). The roundness and micro marks, for example, is closely linked to the degree of transport of that sediment to its final deposit (Kleesment, 2009).

Like sand, clay can also be characterized by grain configuration, fabric, texture, and growth mechanics (Bohor and Hughes, 1971). All these attributes provide relevant information for a more faithful analysis of the sediment and possible correlations with other materials, such as fossils preserved in shale or other clay rock matrix.

In the work of Kleesment (2009), the use of a tension of 10keV provided a significant visualization of the characteristics and textures present in the sand grains, but without revealing much about depth topography. In the work by Vos et al. (2014), the sand grains analyzed between 15 and 22keV showed very prominent surface characteristics and we can already better observe the topography and depth of the sample. Here it is interesting to observe that the authors made an important proportional correlation between the tension used and the magnification: the smaller one the tension, the smaller the magnification and vice versa. This probably brought the images more sharpness and, consequently, more detail. We observed a similar issue when using x5000 magnification and 10keV tension for the analysis of quartz grains in sand.

5.1.2. Fossil

Despite their heterogeneity, the fossils seem to follow the same pattern as the sediments, where the lowest and uncoated tensions (3, 5 and 10keV) share characteristics related to texture, topography and granulometry of the sample as well as the morphology of the fossils present in the sediment. Higher tensions and coated samples (e.g. Fig. 3; 15 and 20keV in filament networks) can bring us more

information about topography, depth of fossil features. With greater penetration of the electron beam, the tension of 15 and 20keV show us the networks of filaments that, once more superficial, now gain three-dimensionality, in addition to increasing the degree of visualization of the minerals. By increasing the magnification, we can more easily see that the network of filaments in question may actually be the result of microorganisms activity, in this case known as extracellular polymeric substance (EPS), also identified in the work by Osés et al. (2016), but at 10keV. Perhaps if they had used a higher voltage (15 or 20keV) they could see additional elements that composed more clearly. In our analysis we have observed Al, Fe and C in the network-like structure using those combined parameters. In the case of Osés et al (2016), they have found only carbon. This shows the importance of testing different tensions, spot sizes and magnifications depending on the aim of the study. Furthermore, the variation in magnification (x5000) allowed a very detailed and clear visualization of the minerals present in the sample (in this case, quartz) that can be characterized in terms of their euhedral geometry in lycopsids fossils. As an example, we can mention two SEM plates (Figures 2 and 3 in Osés et al., 2017) present in the article by Osés et al. (2017) where some images at 3, 5 and 10keV tensions reinforce our hypothesis, even for one of the 10keV images with x5000 magnification, where the structure is quite sharp.

In the case of Lontras Shale, the insect's muscle (which was not coated), preserved in clay sediment, seems to have suffered more from charging, mainly at lower (3keV) and high (15 and 20keV) tensions, having as based on our results obtained with pure clay.

5.2. Energy Dispersive Spectroscopy (EDS) and Synchrotron Micro-X-Ray-Fluorescence (μXRF)

5.2.1. Sediment

We can say, in general, that EDS and μXRF act in a complementary way when it comes to elemental mapping analysis. This is because the limitations of EDS are overcome by μXRF and vice versa, as our results have already shown. The EDS of the analyzed sediments show the predominance of the basic components of pure clay and sand, becoming more intense as the tension increases, both in the coated

and uncoated samples. However, the coated sediments proved to be more efficient in detecting the basic elements and, at high tensions, they were also more efficient in the detection of other elements such as C and Al. However, if the researcher's idea is to map the more superficial elements, uncoated samples and at low tensions can also be useful.

Specifically, sigma (confidence interval), it is important because some elements are more susceptible to being detected at certain tensions than at others, so if there is interest in specific elements, the ideal is to be aware of the tensions as well as the coat of the sample.

5.2.2. Fossil

Analytical tests showed that the parameters used for SEM/EDS on pure substrates (clay and sand) can be applied to the study of fossils in corresponding preservation contexts, as is the case here with the silicified lycopsid and insect preserved in shales. The use of low tensions (3, 5 and 10keV) proved to be important in the characterization of surface structures and textures, as well as elements distributed in the most superficial part of the samples. The higher tensions were important mainly in the detection of trace elements (e.g. Ti, Sr). Our results corroborate other analytical studies that also reinforce the importance of combining different parameters in SEM/EDS for a more detailed chemical characterization of fossils (Orr et al., 2009). However, our contribution innovates by testing different analytical parameters, in a systematic way, considering different pure substrates and applications in fossils under correlated preservation contexts. When analyzing elemental mapping techniques such as EDS and μXRF, we can observe that, with increasing tension, there is a greater detection of elements in the case of EDS. And μXRF supports heavier trace element detection. However, despite the same purpose, the techniques converge in some aspects: EDS can cover a large number of elements, both light and heavy.

μXRF, as it is a more sophisticated technique, covers heaviest elements and rare earth elements (REE), often present as trace elements. Thus, the use of the two techniques complement each other and end up producing a more robust analysis. It is also necessary to remember that, in the case of EDS, there is a confidence

interval, the sigma, which must be considered in the final result since only the mapping can give a false presentation of some elements. In this context, we can improve our investigations in the samples and explore in a more independent and oriented way to what we are looking for. In the case of fossils, more accurate information about the anatomy, the deposition environment and paleoecological and paleoenvironmental aspects can be described through models using these techniques (e.g. Becker-Kerber et al., 2017; 2020; 2021; Mouro et al., 2020; Osés et al., 2016; 2017).

Specifically regarding EDS, Orr, Kearns and Briggs (2009) discussed the importance of testing different tensions between 5 and 20keV, as well as their relationship with sample depth, in the search for carbon cuticles and their role in fossil preservation of the Burgess Shale. In the case of μXRF, Gueriau and Bertrand (2015) explore the use of the technique in paleontology and discuss its methodology showing how μXRF can be important to observe anatomical details and information about the burial site of the organism.

5.3. Cathodoluminescence (CL)

Hot cathodoluminescence is a widely used low-cost technique to assess the composition, contact/inclusion relationships, different mineral generations, crystallographic zonation, relicts, or overgrowth of minerals, and evaluate recrystallization of bioclasts and carbonates (Budd et al., 2000; Bernet and Basset, 2005; Götze and Kempe, 2008; Oliveira et al., 2018). Furthermore, the luminescence of siliciclastic grains, especially quartz, is applied in studies of sedimentary provenance (Omer, 2015). In experimental works, such as this one, cathodoluminescence analyzes can be used to (1) verify the homogeneity of the sediments used as substrate; (2) recognize the presence of iron oxide films, organic matter, or diagenetic phases on the edges of the grains; (3) identify mineral inclusions, fluid inclusions, and compositional zoning; (4) indicate relic overgrowth and dusty lines; and (5) confirm the degree of roundness/angularity of the grains since this characteristic can be modified by eo- and mesodiagenetic processes.
Specifically, for this work, it is noted that the analyzed samples present homogeneous composition and color, defining the same origin for the quartz grains.

However, it is possible to notice the presence of iron films on the edges of some grains, which may indicate the need for prior treatment with hydrochloric acid.

Additionally, scattered luminescent spots on the grains and matrix probably reflect dust accumulated in the resin used for the impregnation of the slide or deposited during sample preparation. It is also possible to identify that the grains do not present major physical changes, for example, longitudinal fracturing, fragmented grains, or shell fractures occur very rarely. The analyzed sediments present textural modifications caused by transport, which are highlighted by cathodoluminescence signatures (e.g., Oliveira et al., 2018). These modifications include: abrasion edges, percussion marks, dissolve marks, and drag streaks.

Differences in cathodoluminescence properties are better observed if there is a discrepancy in the concentration of certain elements, such as Fe and Mn (Budd et al., 2000). In polymorphs without major textural differences, the presence of distinct mineral phases may go unnoticed. Another limitation is the absence of luminescence in some elements, such as sulfides and ferromagnesian minerals (Götze and Kempe, 2008). Minerals such as pyrite and gypsum are commonly generated during fossildiagenesis (Vogel et al., 2010; Zabini et al., 2012; Osés et al., 2017), but they do not emit a luminescence signal. In these cases, conventional petrography or geochemical analyzes such as XRF and XRD are more indicated. Similarly, detailed compositional and textural aspects of very fine-grained minerals and biofilms are better constrained with SEM/EDS or XRF and XRD data, since the scale of observation in the conventional microscope does not allow to properly evaluate the clay minerals assemblage.

5.4. Micro-Raman Spectroscopy (μRaman) and X-Ray-Diffraction (XRD)

5.4.1. Sediment

Based on our results, we can observe in pure sand the composition rich in quartz (both in μRaman and in XRD) and feldspar in its albite and microcline (XRD) variations. Likewise, clay is supported by quartz (μRaman and XRD), anatase and calcite (μRaman), and pyrophyllite and diaspore (XRD). As they are techniques that seek to understand minerals at the molecular level, they end up complementing each other, since with μRaman we can observe the vibration between molecules, which

can result in the identification of the mineral phase, and with XRD we can observe the crystalline structure of the mineral..

By relating μRaman with SEM-EDS, it is observed that, while SEM-EDS allows us to map and locate elements and molecules within a sample, μRaman gives us a mineralogical context through the phases of the mineral (Fries and Steele, 2018). If SEM-EDS tells us, for example, silicon oxide (SiO2) in a given sample, μRaman can tell us, among other things, which phase this silica is in (e.g. quartz, cristobalite) (Fries and Steele, 2018). In this way, we can understand, from the relationship between these techniques, that there really is the presence of a certain element in a certain phase in that sample. Secchi et al. (2018) used this inter-relationship between the techniques to analyze two rock fragments and concluded that the joint use of XRD, XRF, SEM-EDS and μRaman were very useful for the characterization and geochemical interpretation of the samples.

5.4.2. Fossil

When dealing with the lycophyte stem fragment, we noticed that in all samples there is a prevalence of silica in its quartz phase, in addition to calcite and anhydrite. In the Folhelho Lontras insect, it was possible to observe amorphous carbon. In theory, μRaman has a high sensitivity for phases of carbonaceous materials, which explains the calcite peaks present in the lycophyte and the amorphous carbon of the insect. However, much is still being discussed about this, since the carbon present in the samples cannot necessarily be related to organic matter. This subject has gained a lot of visibility due to the use of Raman spectroscopy to search for signs of life and biosignatures in extraterrestrial rock samples. Because of this, the ideal is to contemplate several techniques for a more accurate analysis.

By being able to differentiate crystal phases, μRaman can help different areas in different ways. An example from ecology refers to the use of μRaman for the differentiation of calcium carbonate phases in coral skeletons since, due to its sensitivity to climate change, it can provide relevant information about the environment (DeCarlo, 2018).

6. Conclusions

Given the comparisons made here, added to other studies on the fossil record, we consider that the most adequate characterization of fossils and other geological materials should follow, as far as possible, the following recommendations:

(1) Clarity of purposes and objectives about the sample under study;

(2) Rigorous testing of parameters (in observational and experimental approaches);

(3) The use of analytical techniques that present well known complementarity and limitations, leading to standardization and systematization of data access;

(4) Use of data collection techniques and compilation forms that serve as calibration for comparative purposes.

More specifically, we note the following points regarding the techniques used in this study:

(1) Elementary and classical imaging techniques, such as MEV/EDS are still the most recommended for exploratory studies, or even initial characterizations of geological samples. A good initial imaging is able to reveal data not only about the topography and depth of morphological microstructures, but also can indicate the presence of important minerals to be investigated by the means of more sensitive techniques, such as XRF and micro-Raman.

(2) Elementary techniques such as EDS and XRF are perfectly complementary. XRF is more sensitive to trace elements and REE, but its detection limit is adjustable only to elements heavier than silicon. EDS, on the other hand, is able to detect intensities of almost every element in the periodic table, but it is less sensitive to trace elements.

(3) A definition of the study purpose counts very much in favor of the analytical parameters to be considered:

(A) Studies aimed at characterizing organic matter in fossils, for example, should take into account good imaging, by the means of SEM and cathodoluminescence, combined with the use of vibrational techniques, such as micro-Raman, for the mapping of heterogeneities.

(B) Studies aimed at mineralogical characterization, on the other hand, must take into account the use of vibrational techniques (bearing in mind the appropriate choice of laser as a function of fluorescence and luminescence) and X-ray diffraction. Raman spectroscopy is more sensitive in detecting minerals and is less destructive or invasive. XRD, on the other hand, is less sensitive than micro-Raman, being, in most cases, destructive due to sample processing. However, a larger volume of sample can be taken into account in the diffractogram results.

(4) Exploratory study and testing of parameters on pure substrates, such as sand and clay, can be very useful in the decomposition of variables – and can also serve as comparisons with rock substrates in which fossils are preserved.

(5) Some techniques can be beyond complementary: they can be calibrating. In our studies, we observed that XRD was very useful in identifying illite bands that were skewed by the luminescence phenomenon of the sample submitted to micro-Raman.

CRediT authorship contribution statement

Natália Cantuária: Formal analysis, Investigation, Data Curation, Writing - Original Draft; **Lucas D. Moro**: Formal analysis, Data Curation; **Mírian L. A. F. Pacheco**: Conceptualization, Software, Validation, Formal analysis, Investigation, Data Curation, Resources, Writing - Original Draft, Writing - Review & Editing, Supervision, Project administration, Funding acquisition.

Acknowledgments

We would like to thank José Carlos “Satílio” and other citizen scientists from Angatuba, SP, for finding some of the fossils from this work, as well as the owner of the property, Fernando de Moraes Turele. We would like to thank the *Programa de Pós-Graduação em Ecologia e Recursos Naturais* (PPGERN-UFSCar). Thank you to Gabriel Barros and Gabriel Romano for helping with the design of images and

graphs. Thank you to João Ricetti for providing images and data from Lontras Shale. Thank you to Fabio Rodrigues for processing XRD samples. Guilherme Popts for helping with SEM/EDS and XRF analysis. To Flavia Callefo for helping with synchronton analysis. To Alisson Martins for helping with analysis and the paper's draft. To Márcia Rizzutto for providing XRF analysis. The Ouro Branco company for donating the clay used in this work. The *Laboratório de Catodoluminescência a*nd Alexandre Ribeiro from Federal University of Pará (UFPA) for the cathodoluminescence analysis. *Laboratório da Quimiosfera* for the Raman analysis. *Laboratório de Plasmas Tecnológicos* (LaPTec Unesp - Sorocaba campus)and Elidiane Rangel and the *Centro de Estudos em Petrologia e Geoquímica* of the Federal University of Rio Grande do Sul (UFRGS) for SEM/EDS analysis. *Instituto de Geociências* (IGc) of the University of São Paulo (USP - Butantã campus) for the XRD analysis. The Brazilian Center for Research in Energy and Materials (CNPEM) for the XRF analysis. We would like to thank the Coordination for the Improvement of Higher Education Personnel (CAPES) of Brazil - Finance Code 001, master´s grant awarded to N.C. (process number 88882.426386/2019-01).

References

Barros, O.A., Silva, J.H., Saraiva, G.D., Viana, B.C., Paschoal, A.R., Freire, P.T.C., Oliveira, N.C., Paula, A.J., Viana, M.S., 2019. Physicochemical investigation of shrimp fossils from the Romualdo and Ipubi formations (Araripe Basin). PeerJ, 7, e6323.

Becker-Kerber, B., Osés, G.L., Curado, J.F., Rizzutto, M.D.A., Rudnitzki, I.D., Romero, G.R., Onary-Alves, S.Y., Benini, V.G., Galante, D., Rodrigues, F., Buck, P.V., Rangel, E.C., Ghilardi, R.P., Pacheco, M.L.A.F., 2017. Geobiological and Diagenetic Insights from Malvinokaffric Devonian Biota (Chapada Group, Paraná Basin, Brazil): Paleobiological and Paleoenvironmental Implications. Palaios, 32(4), 238-249.

Becker-Kerber, B., Paim, P.S.G., Junior, F.C., Girelli, T.J., da Rosa, A.L.Z., El Albani, A., Osés, G.L., Prado, G.M.E.M., Figueiredo, M., Simões, L.S.A.,

Pacheco, M.L.A.F., 2020. The oldest record of Ediacaran macrofossils in Gondwana (~ 563 Ma, Itajaí Basin, Brazil). Gondwana Research, 84, 211-228.

Becker-Kerber, B., El Albani, A., Konhauser, K., Abd Elmola, A., Fontaine, C., Paim, P.S.G., Mazurier, A., Prado, G.M.E.M., Galante, D., Kerber, P.B., da Rosa, A.L.Z., Fairchild, T.R., Meunier, A., Pacheco, M.L.A.F., 2021. The role of volcanic-derived clays in the preservation of Ediacaran biota from the Itajaí Basin (ca. 563 Ma, Brazil). Scientific reports, 11(1), 1-10.

Bernet, M., Bassett, K., 2005. Provenance analysis by single-quartz-grain SEM-CL/optical microscopy. Journal of Sedimentary Research, 75(3), 492-500.

Bertrand, L., Schöeder, S., Anglos, D., Breese, M.B., Janssens, K., Moini, M., Simon, A., 2015. Mitigation strategies for radiation damage in the analysis of ancient materials. TrAC Trends in Analytical Chemistry, 66, 128-145.

Brasier, M.D., Wacey, D., 2012. Fossils and astrobiology: new protocols for cell evolution in deep time. International Journal of Astrobiology, 11(4), 217.

Budd, D.A., Hammes, U., Ward, W.B., 2000. Cathodoluminescence in calcite cements: new insights on Pb and Zn sensitizing, Mn activation, and Fe quenching at low trace-element concentrations. Journal of Sedimentary Research, 70(1), 217-226.

DeCarlo, T. M. 2018. Characterizing coral skeleton mineralogy with Raman spectroscopy. Nature Communications, 9:5325.

de Faria, R.S., Ricardi-Branco, F., Giannini, P.C.F., Sawakuchi, A.O., Del Bem, L.E.V. 2009. *Lycopodiopsis derbyi* Renault from the Corumbataí Formation in the state of São Paulo (Guadalupian of Paraná Basin, Southern Brazil): New data from compressed silicified stems. Review of Palaeobotany and Palynology, 158(1-2), 180-192.

Delgado, A.D.O., Buck, P.V., Osés, G.L., Ghilardi, R.P., Rangel, E.C., Pacheco, M.L.A.F., 2014. Paleometry: a brand new area in Brazilian science. Materials Research, 17(6), 1434-1441.

Dias, J.J., Carvalho, I.S., 2020. Remarkable fossil crickets preservation from Crato Formation (Aptian, Araripe Basin), a Lagerstätten from Brazil. Journal of South American Earth Sciences, 98, 102443.

Dodd, M.S., Papineau, D., Grenne, T., Slack, J.F., Rittner, M., Pirajno, F., O'Neil, J., Little, C.T., 2017. Evidence for early life in Earth's oldest hydrothermal vent precipitates. Nature, 543(7643), 60-64.

Foucher, F., 2019. Detection of biosignatures using Raman spectroscopy. In: Biosignatures for Astrobiology (pp. 267-282). Springer, Cham.

Fries, M., Steele, A. 2018. Raman spectroscopy and confocal Raman imaging in mineralogy and petrography. In: Toporski J., Dieing T., Hollricher O. (eds) Confocal Raman Microscopy. Springer Series in Surface Sciences, vol 66.

Fúlfaro, V. J. 1970. Contribuição à geologia da região de Angatuba, Estado de São Paulo (Doctoral dissertation, Universidade de São Paulo).

Gomes, A.L., Becker-Kerber, B., Osés, G.L., Prado, G., Kerber, P.B., De Barros, G.E.B., Galante, D., Rangel, E., Bidola, P., Herzen, J., Pfeiffer, F., Rizzutto, M.A., Pacheco, M.L.A.F., 2019. Paleometry as a key tool to deal with paleobiological and astrobiological issues: some contributions and reflections on the Brazilian fossil record. International Journal of Astrobiology, 18(6), 575-589.

Götze, J., Kempe, U. 2009. Physical principles of cathodoluminescence (CL) and its application in geosciences. In: Cathodoluminescence in geosciences. Pagel M., Barbin V., Blanc Ph., Ohnenstetter D. (Eds.). Springer. 1-22p.

Grazulis, S., Chateigner, D., Downs, R.T., Yokochi, A.T., Quiros, M., Lutterotti, L., Manakova, E., Butkus, J., Moeck, P., Le Bail, A., 2009. Crystallography

Open Database – an open-access collection of crystal structures. Journal of Applied Crystallography, 42, 726-729.

Grotzinger J. P. 2014. Habitability, taphonomy, and the search for organic carbon on Mars. Science 343, 386–387.

Gueriau, P., Bertrand, L., 2015. Deciphering exceptional preservation of fossils through trace elemental imaging. Microscopy Today, 23(3), 20-25.

Gueriau, P., Jauvion, C., Mocuta, C., 2018. Show me your yttrium, and I will tell you who you are: implications for fossil imaging (Vol. 61, No. 6, pp. 981-990).

Gueriau, P., Réguer, S., Leclercq, N., Cupello, C., Brito, P.M., Jauvion, C., Morel, S., Charbonnier, S., Thiaudière, D., Mocuta, C., 2020. Visualizing mineralization processes and fossil anatomy using synchronous synchrotron X-ray fluorescence and X-ray diffraction mapping. Journal of the Royal Society Interface, 17(169), 20200216.

Hutchinson, I. B., Ingley, R., Edwards, H. G., Harris, L., McHugh, M., Malherbe, C., & Parnell, J. 2014. Raman spectroscopy on Mars: identification of geological and bio-geological signatures in Martian analogues using miniaturized Raman spectrometers. Philosophical Transactions of the Royal Society A: Mathematical, Physical and Engineering Sciences, 372(2030), 20140204.

Iniesto, M., Villalba, I., Buscalioni, A. D., Guerrero, M. C., López-Archilla, A.I., 2017. The effect of microbial mats in the decay of anurans with implications for understanding taphonomic processes in the fossil record. Scientific reports, 7(1), 1-12.

Iniesto, M., Blanco-Moreno, C., Villalba, A., Buscalioni, Á.D., Guerrero, M.C., López-Archilla, A.I., 2018. Plant tissue decay in long-term experiments with microbial mats. Geosciences, 8(11), 387.

Iniesto, M., Gutiérrez-Silva, P., Dias, J.J., Carvalho, I.S., Buscalioni, A.D., López-Archilla, A.I., 2021. Soft tissue histology of insect larvae decayed in laboratory experiments using microbial mats: Taphonomic comparison with Cretaceous fossil insects from the exceptionally preserved biota of Araripe, Brazil. Palaeogeography, Palaeoclimatology, Palaeoecology, 564, 110156.

Kleesment, A., 2009. Roundness and surface features of quartz grains in Middle Devonian deposits of East Baltic and their palaeogeographical implications. Estonian Journal of Earth Sciences, 58, 1, 71-84.

Krinsley, D., Margolis, S., 1968. A study of quartz sand grain surface textures with the scanning electron microscope. Transactions New York Academy of Sciences, Section of Geological Sciences.

Lafuente, B., Downs R.T., Yang, H., Stone, N., 2015. The power of databases: the RRUFF project. In: Highlights in Mineralogical Crystallography, T Armbruster and R M Danisi, eds. Berlin, Germany, W. De Gruyter, pp 1-30.

Marshall, A., Marshall, C.P., 2015. Vibrational spectroscopy of fossils. Palaeontology, 58(2), 201-211.

Mouro, L.D., Pacheco, M.L.A.F., Ricetti, J.H., Scomazzon, A.K., Horodyski, R.S., Fernandes, A.C., Carvalho, M.A., Weinschutz, L.C., Silva, M.S., Waichel, B.L., Scherer, C. M., 2020. Lontras Shale (Paraná Basin, Brazil): Insightful analysis and commentaries on paleoenvironment and fossil preservation into a deglaciation pulse of the Late Paleozoic Ice Age. Palaeogeography, Palaeoclimatology, Palaeoecology, 555, 109850.

Oliveira, C.E.S., Pe-Piper, G., Piper, D.J.W., Zhang, Y., Corney, R., 2017. Integrated methodology for determining provenance of detrital quartz using optical petrographic microscopy and cathodoluminescence (CL) properties. Marine and Petroleum Geology, 88, 41-53.

Omer, M.F., 2015. Cathodoluminescence petrography for provenance studies of the sandstones of Ora Formation (Devonian-Carboniferous), Iraqi Kursditan Region, northern Iraq. Journal of South African Earth Sciences, 109: 195-210.

Orr, P.J., Kearns, S.L., Briggs, D.E., 2009. Elemental mapping of exceptionally preserved 'carbonaceous compression' fossils. Palaeogeography, Palaeoclimatology, Palaeoecology, 277(1-2), 1-8.

Osés, G.L., Petri, S., Becker-Kerber, B., Romero, G.R., Rizzutto, M.A., Rodrigues, F., Galante, D., da Silva, T.F., Curado, J.F., Rangel, E.C., Ribeiro, R.P., Pacheco, M.L.A.F., 2016. Deciphering the preservation of fossil insects: a case study from the Crato Member, Early Cretaceous of Brazil. PeerJ, 4, e2756.

Osés, G.L., Petri, S., Voltani, C.G., Prado, G.M., Galante, D., Rizzutto, M.A., Rudnitzki, I.D., da Silva, E.P., Rodrigues, F., Rangel, E.C., Sucerquia, P.A., Pacheco, M.L.A.F., 2017. Deciphering pyritization-kerogenization gradient for fish soft-tissue preservation. Scientific Reports, 7(1), 1-15.

Orosei, R., Lauro, S.E., Pettinelli, E., Cicchetti, A., Coradini, M., Cosciotti, B., Di Paolo, F., Flamini, E., Mattei, E., Pajola, M., Soldoviere, F., Cartacci, M., Cassenti, F., Frigeri, A., Giuppi, S., Martufi, R., Masdea, A., Mitri, G., Nenna, C., Noschese, R., Restano, M., Seu, R., 2018. Radar evidence of subglacial liquid water on Mars. Science, 361(6401), 490-493.

Prado, G., Arthuzzi, J.C., Osés, G.L., Callefo, F., Maldanis, L., Sucerquia, P., Becker-Kerber, B., Romero, G.R., Quiroz-Valle, F.R., Galante, D., 2021. Synchrotron radiation in palaeontological investigations: Examples from Brazilian fossils and its potential to South American palaeontology. Journal of South American Earth Sciences, 102973.

Riquelme, F., Ruvalcaba-Sil, J.L., Alvarado-Ortega, J., 2009. Palaeometry: Non-destructive analysis of fossil materials. Boletín de la Sociedad Geológica Mexicana, 61(2), 177-183.

Sallun Filho, W., Ghilardi, R.P., Silva, L.H.S., Hachiro, J., 2012. Permian stromatolites associated with bivalve coquina beds—Angatuba, SP, Brazil (Teresina Formation, Paraná Basin). Palaeontol. Electron., 15, 1-16.

Schopf, J.W., Farmer, J.D., Foster, I.S., Kudryavtsev, A.B., Gallardo, V.A., Espinoza, C., 2012. Gypsum-permineralized microfossils and their relevance to the search for life on Mars. Astrobiology, 12(7), 619-633.

Secchi, M., Zanatta, M., Borovin, E., Bortolotti, M., Kumar, A., Giarola, M., Sanson, A., Orberger, B., Daldosso, N., Gialanella, S., Mariotto, G., Montagna, M., Lutterotti, L. 2018. Mineralogical investigations using, XRD, XRF and Raman spectroscopy in a combined approach. Journal of Raman Spectroscopy, 1-8.

Sepkoski, D., 2008. Evolutionary paleontology and the fossil record: a historical introduction. The Paleontological Society Papers, 14, 41-53.

Simões, M.G., Torello, F.D.F., Rocha-Campos, A.C., 1996. Gênese e classificação da coquina de Camaquã, Formação Corumbataí (Neopermiano), na região de Rio Claro, SP. Anais da Academia Brasileira de Ciências, 543-557.

Simões, M.G., Torello, F.F., 2003. Modelo de tafofácies para os moluscos bivalves do Grupo Passa Dois (Formações Serra Alta, Teresina e Corumbataí), Permiano superior, Bacia do Paraná, Brasil. Revista Brasileira de Geociências, 33(4), 371-380.

Spiekermann, R., André, J., Benício, J.R.W., Margot, G.S., Soledad, R.B.F., Dieter, U., 2020. Late Palaeozoic lycopsid macrofossils from the Paraná Basin, South America–An overview of current knowledge. Journal of South American Earth Sciences, 102615.

Trueman, C.N., 2013. Chemical taphonomy of biomineralized tissues. Palaeontology, 56(3), 475-486.

Vogel, M.B., Des Marais, D.J., Parenteau, M.N., Jahnke, L.L., Turk, K.A., Kubo, M.D.Y., 2010. Biological influences on modern sulfates: Textures and composition of gypsum deposits from Guerrero Negro, Baja California Sur, Mexico. Sedimentary Geology 223, 265-280.

Vos, K., Vandenberghe, N., Elsen, J., 2014. Surface textural analysis of quartz grains by scanning electron microscope (SEM): From sample preparation environmental interpretation. Earth-Science Reviews 128, 93-104.

Wickham, H., 2011. ggplot2. Wiley Interdisciplinary Reviews: Computational Statistics 3, 180–185.

Zabini, C., Schiffbauer, J.D., Xiao, S., Kowalewski, M., 2012. Biomineralization, taphonomy, and diagenesis of Paleozoic lingulide brachiopod shells preserved in silicified mudstone concretions. Palaeogeography Palaeoclimatology Palaeoecology, 326–328, 118–127.

ANEXO I: Submissão do artigo

Journal of South American Earth Sciences

Purposes and choices on the characterization of fossil samples: parameter tests and analytical techniques applied to the comparison of different substrates

--Manuscript Draft--

Manuscript Number:	
Article Type:	Research Paper
Keywords:	Paleometry; Methodologies in paleontology; Paleontological data
Corresponding Author:	Natália Cantuária BRAZIL
First Author:	Natália Cantuária
Order of Authors:	Natália Cantuária
	Lucas Moro
	Mírian Liza Alves Forancelli Pacheco
Abstract:	Historically, paleontology has been concerned with observational and explanatory issues regarding fossils. However, with the advancement of science and technology, a new field has been structured within this area: paleometry. This interdisciplinary effort seeks to understand how we can use a bulk of techniques in order to access information and interpret data on fossil record. The understanding of limitations and complementarities among techniques can clarify purposes and choices in paleontological research. Despite its contribution, paleometry as a science still needs to be further developed in technical terms. This article aims to present some results of tests of different analytical techniques, under different parameters, in the analysis of sediments, rocks, and fossils.
Suggested Reviewers:	Gabriel Osés gabriel.ladeiraoses@gmail.com
	Douglas Galante douglas.galante@lnls.br
	Paula Sucerquia psucerquia@gmail.com
	Guilherme Romero graffaeli@gmail.com
Opposed Reviewers:	

ANEXO II: Colunas estratigráficas da Formação Corumbataí

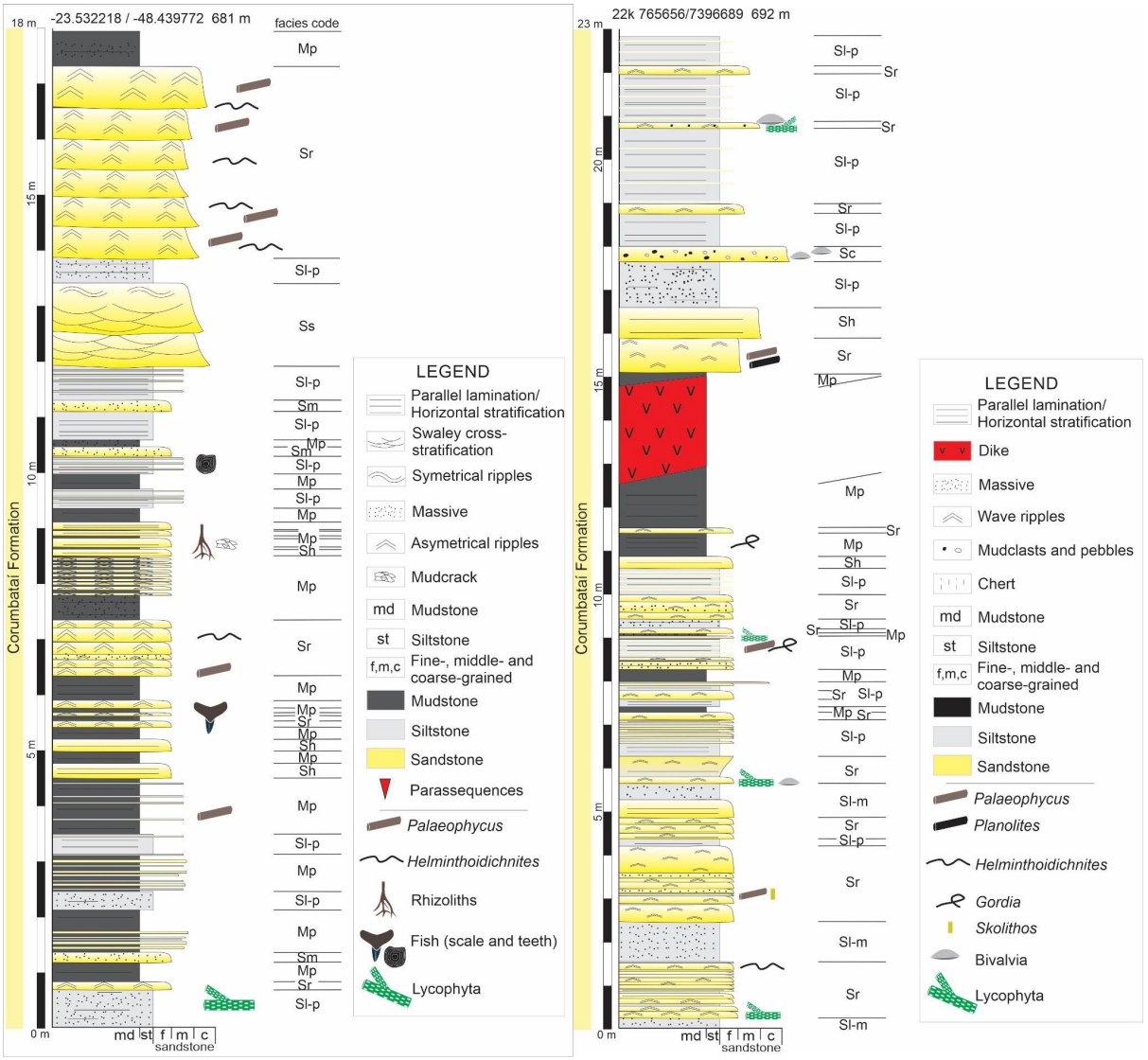

Colunas estratigráficas produzidas por Dr. Daniel Sedorko

ANEXO III: Caracterização de fácies da Formação Corumbataí

Facies

Code	texture	primary sedimentary structures	biogenic sedimentary structures	bioturbation degree	fossil content
Mp	Mudstone locally interbedded to fine- to medium-grained sandstone lenses	Massive to incipient parallel lamination, sandstone lenses with asymmetrical ripples, locally with mudcrack	*Palaeophycus,* rhizoliths	0	-
Sl-p	siltstone interbedded to very fine-grained sandstone lenses	massive to incipient parallel lamination	-	0	Lycopsids; fish scales
Sl-m	siltstone interbedded to very fine-grained sandstone lenses	massive	*Palaeophycus, Helminthoidichnites*	1	-
Sr	fine-grained sandstone with carbonate cementation	Asymmetrical ripples	*Palaeophycus, Planolites, Helminthoidichnites, Skolithos*	1-2	xenacanthids teeths; lycopsids; mollusk bivalve
Ss	fine-grained sandstone	Swaley cross-stratification locally with symmetrical ripples	-	0	-
Sm	silicified fine-grained sandstone	massive	-	0	-

Sh	fine-grained sandstone	Horizontal stratification	-	0	-
Sc	Coarse-grained sandstone	massive	-	0	mollusk bivalve

Tabela produzida por Dr. Daniel Sedorko